



HAL
open science

Involvement of caspase-1 in inflammasomes activation and bacterial clearance in *S. aureus*-infected osteoblast-like MG-63 cells

Elma Lima Leite, Arthur Gautron, Martine Deplanche, Aurélie Nicolas, Jordane Ossemond, Minh-Thu Nguyen, Fillipe L. R. Do Carmo, David Gilot, Vasco Azevedo, Friedrich Goetz, et al.

► To cite this version:

Elma Lima Leite, Arthur Gautron, Martine Deplanche, Aurélie Nicolas, Jordane Ossemond, et al.. Involvement of caspase-1 in inflammasomes activation and bacterial clearance in *S. aureus*-infected osteoblast-like MG-63 cells. *Cellular Microbiology*, 2020, 22 (8), pp.e13204. 10.1111/cmi.13204 . hal-02565096

HAL Id: hal-02565096

<https://univ-rennes.hal.science/hal-02565096>

Submitted on 14 May 2020

HAL is a multi-disciplinary open access archive for the deposit and dissemination of scientific research documents, whether they are published or not. The documents may come from teaching and research institutions in France or abroad, or from public or private research centers.

L'archive ouverte pluridisciplinaire **HAL**, est destinée au dépôt et à la diffusion de documents scientifiques de niveau recherche, publiés ou non, émanant des établissements d'enseignement et de recherche français ou étrangers, des laboratoires publics ou privés.

**Involvement of caspase-1 in inflammasomes activation and bacterial clearance
in *S. aureus*-infected osteoblasts-like MG-63 cells.**

Elma Lima Leite^{1,2}, Arthur Gautron³, Martine Deplanche¹, Aurelie Nicolas¹, Jordane Ossemond¹, Minh Thu Nguyen ⁴, Fillipe L. R. do Carmo^{1 2}, David Gilot³, Vasco Azevedo², Friedrich Goetz⁵, Yves Le Loir¹, Michael Otto⁶, Nadia Berkova¹

¹ Institut National de la Recherche Agronomique, Unité Mixte de Recherche 1253 STLO, Rennes, France; Agrocampus Ouest, Unité Mixtes de Recherche 1253 STLO, Rennes, France.

² Instituto de Ciências Biológicas - Universidade Federal de Minas Gerais, Belo Horizonte- Minas Gerais, Brazil.

³ Univ Rennes, CNRS, IGDR [(Institut de génétique et développement de Rennes)]-UMR 6290, F-35000, Rennes, France.

⁴ Paul-Ehrlich-Institute, Federal Regulatory Agency for Vaccines and Biomedicines, Langen 63225, Germany

⁵ Mikrobielle Genetik, Universität Tübingen, D-72076 Tübingen, Germany

⁶ Laboratory of Human Bacterial Pathogenesis, US National Institutes of Health, Bethesda, Maryland, 20892, USA.

Correspondence : Dr. Nadia Berkova

nadejda.berkova@inra.fr

Running title: Bacterial clearance in osteoblasts-like cells

Abstract

Staphylococcus aureus, a versatile Gram-positive bacterium, is the main cause of bone and joint infections (BJI), which are prone to recurrence. The inflammasome is an immune signaling platform that assembles after pathogen recognition. It activates proteases, most notably caspase-1 that proteolytically matures and promotes the secretion of mature IL-1 β and IL-18. The role of inflammasomes and caspase-1 in the secretion of mature IL-1 β and in the defence of *S. aureus*-infected osteoblasts has not yet been fully investigated. We show here that *S. aureus*-infected osteoblast-like MG-63 but not caspase-1 knock-out *CASP1*^{-/-}MG-63 cells, which were generated using CRISPR-Cas9 technology, activate the inflammasome as monitored by the release of mature IL-1 β . The effect was strain-dependent. The use of *S. aureus* deletion and complemented phenole soluble modulins (PSMs) mutants demonstrated a key role of PSMs in inflammasomes-related IL-1 β production. Furthermore, we found that the lack of caspase-1 in *CASP1*^{-/-}MG-63 cells impairs their defense functions, as bacterial clearance was drastically decreased in *CASP1*^{-/-}MG-63 compared to wild-type cells. Our results demonstrate that osteoblast-like MG-63 cells play an important role in the immune response against *S. aureus* infection through inflammasomes activation and establish a crucial role of caspase-1 in bacterial clearance.

Key words: Staphylococcus aureus, inflammasomes, caspase-1, CRISPR-Cas9 gene editing, bacterial clearance.

Introduction

Staphylococcus aureus is a highly adaptive and versatile Gram-positive bacterium that has major importance for human and animal health (Liu, 2009). *S. aureus* causes diseases ranging from minor skin infections to life-threatening infections such as bacteremia, pneumonia, meningitis, endocarditis and sepsis (Tong *et al.*, 2015). *S. aureus* is also the main cause of bone and joint infections (BJI), particularly in the presence of orthopedic devices (Kahl *et al.*, 2016). Despite adequate antimicrobial therapy BJI are linked to a high percentage of relapse, often leading to the development of a chronic disease demanding particularly challenging treatments (Del Pozo and Patel, 2009). While research into treatment options has been focused mostly on antibacterial strategies, it is widely believed that treatment of recurrent *S. aureus* infections would also benefit considerably from the reinforcement of host defenses (Valour *et al.*, 2015), and a deeper understanding of the immune response is crucial for the development of new anti-infective strategies.

The innate immune response plays a crucial role in the defense against pathogens and is initiated through pattern recognition receptors (PRRs), which recognize microbial

pathogen-associated molecular patterns (PAMPs) and endogenous danger-associated molecular patterns (DAMPs) (Rivera *et al.*, 2016). This leads to the activation of host defense pathways that results in the clearance of infections. The innate immune response against microbes involves a major inflammatory pathway known as the activation of inflammasomes, multi-protein signaling complexes that assemble after recognition of danger signals and/or pathogens (Schroder and Tschopp, 2010). Inflammasomes consist of a family of cytosolic receptors called NLRs (nucleotide binding domain and leucine rich repeats containing receptors), PYHIN protein family and enzymatic components, most notably caspase-1 (canonical inflammasomes) and less frequently caspase-11 in mice (Broz and Dixit, 2016) or caspase-4 and -5 in human (non-canonical inflammasomes) (Choi *et al.*, 2019). Caspase-1 is synthesized in cells as an inactive precursor of 45 kDa that is matured into two subunits of 20 and 10 kDa after inflammasome activation (Lamkanfi and Dixit, 2014). Most inflammasomes also use an adaptor molecule known as ASC (apoptosis-associated speck-like protein) (Mariathasan *et al.*, 2004). After stimulation with pathogens or DAMPS, inflammasome assembly leads to the autocatalytic cleavage of caspase-1, processing of pro-IL-1 β and pro-IL-18 and secretion of mature IL-1 β and IL-18 (Strowig *et al.*, 2012). Furthermore, inflammasome activation may trigger pyroptosis, an inflammatory form of cell death. The role of inflammasomes in the innate immune response against various microbes has been intensively explored (Vladimer *et al.*, 2013; Higa *et al.*, 2013). Special attention has been paid to the investigation of the role of inflammasomes during infection with intracellular pathogens, such as

Salmonella typhimurium, *Legionella pneumophila*, *Listeria monocytogenes* (Amer *et al.*, 2006; Zaki *et al.*, 2014; Maltez *et al.*, 2015; Morales *et al.*, 2017). Many studies also investigated the role of inflammasomes in various types of cells during infection with the facultative intracellular pathogen *S. aureus*: in phagocytes and epithelial cells (Ma *et al.*, 2019; Kremserova and Nauseef, 2019), in human and rat conjunctival goblet cells (McGilligan *et al.*, 2013), in human keratinocytes (Simanski *et al.*, 2016). Additionally, it was reported that the expression of inflammasomes-associated proteins such as the sensor molecule NLRP3 and caspase-1 in infectious bone fragments from patients with osteomyelitis was significantly higher than in uninfected bone. Similarly, in *S. aureus*-induced murine osteomyelitis model, higher expression of these proteins was reported (Zhu *et al.*, 2019). However, the role of inflammasomes, *S. aureus* phenol soluble modulins (PSMs) and caspase-1 in the secretion of mature IL-1 β as well as in the defence of *S. aureus*-infected osteoblasts has not yet been fully investigated. In this study we used human MG-63 osteoblasts-like cells to model the infection of osteoblasts in the context of *S. aureus*-associated bone infections (Wright and Friedland, 2004; Selan *et al.*, 2017). We opted for the establishment of CASP1^{-/-} MG-63 cell line using CRISPR-Cas9 system (see Experimental procedures, Selection of the cell model).

We discovered that in response to *S. aureus* infection, wild-type (WT) osteoblast-like MG-63 cells activate inflammasomes in contrast to CASP1^{-/-}MG-63 cells. Inflammasome activation was monitored by caspase-1 activation and the release of mature soluble IL-1 β . Mutant *S. aureus* strains were employed, demonstrating a key

Accepted Article

contribution of PSMs in triggering the release of soluble IL-1 β , which is strongly implicated in the pathology of BJI (Lee *et al.*, 2010). In addition to the key role of caspase-1 in the release of pro-inflammatory cytokines in infected osteoblasts-like cells, we demonstrated that caspase-1 is implicated in cell defense mechanism such as a restriction of the intracellular replication of *S. aureus* that is critical in the development of the infection.

Results:

Caspase-1 activation and IL-1 β release triggered by inflammasome activators in human osteoblasts-like MG-63 cells and THP-1 cells

In order to monitor inflammasome activation in the human osteoblast-like MG-63 cells the detection of active caspase-1 by Western blot analysis was set up in samples containing cells and cell supernatants. As shown in Fig. 1A, exposing MG-63 cells to LPS+ATP, two well-known inflammasomes activators, led to the detection of a 20 kDa band corresponding to the active caspase-1 p20 fragment. The activation of caspase-1 was associated with the production of IL-1 β , as the exposure of cells to LPS+ATP resulted in the production of mature IL-1 β 6 h post-infection (Fig.1B). These results suggest that MG-63 cells form functional inflammasomes and that their activation can be estimated by IL-1 β release.

To compare the ability of inflammasome activation by professional versus non-professional phagocytes, PMA (phorbol 12-myristate 13-acetate)-treated THP1 cells

differentiated into macrophages or MG-63 osteoblast-like cells, were exposed to LPS+ATP and the level of IL-1 β production was estimated at 2 h and 6 h after the beginning of the treatment. PMA-treated control THP1 cells produce ~ 7 pg/mL of IL-1 β 2 h after the beginning of the treatment. Exposure of PMA-differentiated THP-1 cells to LPS+ATP resulted in a significant increase in IL-1 β secretion, up to ~ 30 pg/mL, 2 h post treatment. After 6 h, PMA-treated control THP-1 cells produce ~ 10 pg/mL of IL-1 β , while the level of IL-1 β produced by PMA-treated THP-1 cells after an exposure to LPS+ATP was ~ 650 pg/mL. In contrast, IL-1 β was not detected 2 h post-treatment while only 5 \pm 0.5 pg/mL of IL-1 β was detected in MG-63 cells 6 h after the exposure to LPS+ATP. Six hours post-treatment, the level of IL-1 β produced by MG-63 cells was low, but significantly above the sensitivity threshold of the detection kit, (2 pg/mL; Invitrogen ELISA kit), and dramatically contrasted with professional phagocytes PMA-treated control THP-1 cells that produce ~ 650 pg/mL of IL-1 β .

Establishment of *CASP1*^{-/-}MG-63 cell line using the CRISPR-Cas9 gene editing system

It has been shown that stimulation is required for IL-1 β transcription and protein expression by MG-63 (Koh *et al.*, 1997), a cell line that is commonly used as a model to study BJI (Kazemzadeh-Narbat *et al.*, 2012). To investigate the role of inflammasomes in *S. aureus*-infected human osteoblast-like MG-63 cells, the establishment of *CASP1*^{-/-}MG-63 cell line was carried out using the CRISPR-Cas9 gene editing system (see Experimental procedures, Selection of the cell model).

There are 6 isoforms of caspase-1 encoded by the *CASP1* gene, located on chromosome 11 (Feng *et al.*, 2004). Caspase-1 alpha and beta are the main transcripts in human cells. To generate *CASP1*^{-/-}MG-63 cells we used a previously validated sgRNA ATTGACTCCGTTATTCCGAA (Schmid-Burgk *et al.*, 2015) (Fig.2). Based on sequences analysis, the sgRNA is predicted to target four Caspase-1 isoforms including alpha and beta. Following lentiviral transduction of sgRNA and puromycin selection, individual clones, which were identified as a result of limiting dilution of puromycin-treated cells, were tested by Western blotting for the lack of the 45-kDa band corresponding to pro-caspase-1. Finally, after the cloning procedure described in Experimental procedures, three clones of *CASP1*^{-/-}MG-63 (G2, B9 and C2 clones originated from three different parental clones) were selected for further analysis. Western blot analysis of WT MG-63 vs *CASP1*^{-/-} MG-63 G2 or *CASP1*^{-/-} MG-63 B9 or *CASP1*^{-/-}MG-63 C3 cells confirmed the lack of pro-caspase-1 in all three *CASP1*^{-/-} MG-63 clones (Fig. 2B).

***S. aureus* invades and persists inside human osteoblast-like MG-63 cells**

We and others showed that *S. aureus* can be internalized and survive within professional phagocytes, such as macrophages (Flannagan *et al.*, 2016), as well as within non phagocytic epithelial cells or osteoblasts (Mohamed *et al.*, 2014; Deplanche *et al.*, 2019). To study the capacity of intracellular *S. aureus* to induce inflammasomes formation in human osteoblasts-like MG-63 cells, we confirmed the presence of intracellular bacteria using transmission electron microscopy (Transmission EM) at

different time points. An examination of electron micrographs of the infected MG-63 cells 45 min post infection reveals the presence of intracellular methicillin-resistant *S. aureus* strain MW2 (USA400), and bacteria that are in close contact with MG-63 cells surface (Fig. 3). Infected host cells treated with lysostaphin and gentamicin as described in Experimental procedures were observed from 6 h post-infection up to 12 days. The presence of only intracellular *S. aureus* was evidenced by Transmission EM (Fig. 3), while no extracellular bacteria were detected by CFU determination when supernatants of infected MG-63 cells treated with antibiotics at different time points (from 6h to 12 days) were analyzed. Bacteria were detected in the cytoplasm of MG-63 cells 6 hours, 3 days, and 12 days post-infection. The kinetics of the infection firstly was carried out using the hypervirulent CA-MRSA strain MW2 (Baba *et al.*, 2002). These experiments allowed the setting up of experimental conditions that ensure the detection of intracellular *S. aureus* in infected cells at the end of the incubation. In a previous work (Bouchard *et al.*, 2013), we found that the adhesion and internalization capacities of the *S. aureus* strain that reproducibly induce mild infection were higher than those of the more virulent strain that caused severe infection. Thus, to ensure a higher number of internalized *S. aureus* with an identical MOI, we used the strain SA113, a naturally agr-deficient *S. aureus* strain, which is reportedly less virulent than the wild type (Iordanescu and Surdeanu, 1976; Periasamy *et al.*, 2012). To confirm the presence of intracellular SA113 inside of the host cells CFU of SA113 recovered from WT MG-63 cells were determined as described in Experimental procedures. The results were presented as Survival rate (%) (Fig. S1). We showed that MW2 and

SA113 strains had comparable survival rates (Fig. S1). We observed that 5 days post-infection the number of internalized bacterial cells was drastically decreased. A very low CFU number was found at the end of experiment.

Inflammasome is involved in the caspase-1 dependent release of IL-1 β by *S. aureus* infected MG-63 cells

Activation of the NLRP3 inflammasome involves the oligomerization of the adaptor protein ASC (apoptosis-associated speck-like protein containing A CARD) into speck-like aggregates (Masumoto *et al.*, 2001). This structure recruits and activates pro-caspase-1, which promotes the maturation of IL-1 β and IL-18.

To ensure that the depletion of Caspase-1 in *CASP1*^{-/-}MG-63 cells does not impair upstream events of inflammasome formation, the level of NLRP3 expression and the formation of ASC specks was analyzed in WT MG-63 and *CASP1*^{-/-}MG-63 clones. NLRP3 mRNA expression was estimated by qPCR. As shown in Fig. 4A the exposure of MG-63 cells or *CASP1*^{-/-} MG-63 G2 clone to inflammasome inducers ATP+nigericin resulted in the increase of NLRP3 expression. NLRP3 protein expression was estimated by FACS using Alexa Fluor® 488-conjugated anti-human NLRP3 antibody and corresponding isotype control antibody. As shown in Fig. 4A, equal NLRP3 mRNA expression levels were observed in WT and *CASP1*^{-/-} MG-63 G2 cells. The exposure of both types of cells to *S. aureus* SA113, an agr-deficient strain widely used in staphylococcal research (Herbert *et al.*, 2010), resulted in similarly increased levels of fluorescence. Mean fluorescence intensity (MFI) increased from 2700 to 3800 in WT

MG-63 cells after *S. aureus* infection, similarly to *CASP1*^{-/-} MG-63 G2 cells, which showed an MFI increase from 2800 to 3900 (Fig. 4B). Similar results were obtained with *CASP1*^{-/-} MG-63 B9 and *CASP1*^{-/-} MG-63 C3 clones (Fig. S2).

Taking into account that both types of cells contain NLRP3 (Fig. 4A), while pro-caspase-1 is present only in WT MG-63 cells (Fig. 2B), we next determined whether an exposure of both cell lines to *S. aureus* SA113 led to the formation of ASC specks. As shown in Fig. 5A, 6 h post-infection WT MG-63 cells form ASC speck (green arrows). An exposure of *CASP1*^{-/-} MG-63 G2 clone to *S. aureus* induced an even higher number of ASC speck-forming cells (green arrows). Quantification of ASC speck forming cells by immunofluorescence microscopy provide an opportunity to analyse the inflammasome activation pathway even in the absence of Caspase-1. Consequently, we analyzed immunofluorescence staining for the adaptor ASC in WT and *CASP1*^{-/-} MG-63 cells. As shown in Fig. 5A, *S. aureus* infection triggered assembly of the ASC specks in the cytosols of WT as well as *CASP1*^{-/-} MG-63 G2 clone (green). The number of ASC speck-forming cells in *CASP1*^{-/-} MG-63 G2 clone was twice as high as that in WT MG-63 cells (Fig. 5B). Similar results were obtained with *CASP1*^{-/-} MG-63 B9 and *CASP1*^{-/-} MG-63 C3 clones (Fig.S3, Fig. S4A).

To understand if the observed difference in the number of ASC-forming cells depends on the amount of intracellular bacteria, CFU of *S. aureus* recovered from WT MG-63 cells and *CASP1*^{-/-}MG-63 clones were determined as described in Experimental procedures. A 50:1 MOI was used in this experiment. As shown in Fig. 5C, 6 h post-infection the number of CFU of *S. aureus* recovered from *CASP1*^{-/-}MG-63 G2 cells

was significantly higher than those recovered from WT MG-63 cells. Similar results were obtained with *CASP1*^{-/-} MG-63 B9 and *CASP1*^{-/-}MG-63 C3 cells (Fig. S4B).

Alltogether our results showing that both WT MG-63 cells and *CASP1*^{-/-}MG-63 clones, express NLRP3 and form ASC specks while only WT MG-63 cells produce IL-1 β following the exposure to inflammasomes inducers or to *S. aureus*, approve the monitoring of IL-1 β produced by both cell lines for the analysis of inflammasomes activation.

It was previously reported that transcripts for IL-1 β and IL-18 were observed after an exposure of mice osteoblasts to *S. aureus*. However, secreted IL-1 β and IL-18 were not detected despite the presence of active caspase-1 (Marriott *et al.*, 2002). To understand whether *S. aureus* activates inflammasomes in human osteoblast-like MG-63 cells, we measured IL-1 β production in WT and *CASP1*^{-/-}MG-63 cells.

The assessment of IL-1 β in WT and *CASP1*^{-/-}MG-63 cells exposed to inflammasomes activators LPS+ATP (Fig. 4C) as well as to *S. aureus* SA113 (Fig. 4D) revealed the lack of IL-1 β production in *CASP1*^{-/-}MG-63 G2 in contrast to WT MG-63 cells.

To clarify the possible role of human osteoblasts in the production of IL-1 β , we analyzed the kinetics (from 2 to 11 days) of IL-1 β production by WT and *CASP1*^{-/-}MG-63 G2 cells exposed to *S. aureus* SA113. As demonstrated in Fig. 6A, the level of IL-1 β increased from day 2 to 11. In contrast, IL-1 β was not detected in supernatants from infected *CASP1*^{-/-}MG-63 G2 cells during the tested period. Similar results were obtained with *CASP1*^{-/-}MG-63 B9 and *CASP1*^{-/-}MG-63 C3 cells (Fig. S5).

To verify whether IL-1 β release by infected osteoblasts-like cells was strain-dependent, we analyzed the kinetics of IL-1 β release by MG-63 cells exposed to different *S. aureus* strains: LAC (USA300), MW2 (USA 400) and SA113. As shown in Fig. 6B, all strains induced IL-1 β release; however, MW2 and LAC induced significantly higher levels of IL-1 β than SA113. IL-1 β was not detected in the supernatants of MG-63 cells exposed to killed bacteria of any of the three strains, suggesting that factors associated with viable bacteria are involved in inflammasome activation.

***S. aureus* PSM toxins are involved in stimulation of IL-1 β release by infected MG-63 cells**

The quorum-sensing system in *S. aureus* known as the accessory gene regulator (Agr) regulates the expression of many virulence factors. Agr regulates the expression of most *S. aureus* toxin genes. Of note, the expression of PSMs encoding genes (PSM α 1 to 4, PSM β 1 and 2, and δ -toxin sometimes called PSM γ) is tightly controlled by the Agr system (Queck *et al.*, 2008; Otto, 2010). It has previously been shown that PSMs stimulate the production of inflammatory cytokines by infected keratinocytes (Syed *et al.*, 2015). Furthermore, our results on the strain dependence of IL-1 β stimulation in MG-63 cells suggested a possible involvement of Agr, since the cells infected with the Agr-defective SA113 strain produced low levels of IL-1 β compared to the cells infected with strains MW2 and LAC (pTX Δ 16), which harbor a functional Agr system. Since Agr tightly controls PSM production in *S. aureus*, these considerations prompted us to investigate the role of PSMs in IL-1 β production by infected MG-63 cells.

Accepted Article

First, we analyzed LAC (USA300) wild-type and its isogenic mutant *LAC Δ psma β hld* (*S. aureus* strain lacking PSM α , PSM β and δ -toxin) for their ability to stimulate the release of IL-1 β . As shown in Fig. 7A, the level of IL-1 β was significantly lower in the supernatants of WT MG-63 cells exposed to *LAC Δ psma β hld* compared to that in the supernatant of WT MG-63 cells exposed to wild-type LAC on days 2 and 5 post-infection. To further investigate which PSMs were involved in the stimulation of IL-1 β release, we used the PSM deletion strain *LAC Δ psma β hld* and complemented strains, expressing either the four PSM α peptides (*LAC Δ psma β hld-pTX Δ α 1-4*), the two PSM β peptides (*LAC Δ psma β hld-pTX Δ β 1-2*), or the δ -toxin (*LAC Δ psma β hld-pTX Δ hld*) and monitored IL-1 β levels in cell supernatants exposed to those strains up to 9 days post-infection. As shown in Fig. 7B, there was a significant decrease in the IL-1 β released by cells exposed to the *LAC Δ psma β hld* strain compared to LAC. Exposure to complemented mutants demonstrated that the release was partially restored when the strains were complemented with PSM α (*LAC Δ psma β hld-pTX Δ α 1-4*), PSM β (*LAC Δ psma β hld-pTX Δ β 1-2*) or δ -toxin (*LAC Δ psma β hld-pTX Δ hld*). However, the difference was statistically significant only when strains were complemented with PSM β (*LAC Δ psma β hld-pTX Δ β 1-2*) at days 7 and 9 or, at earlier time points (days 2 and 5), with both PSM β and PSM α (*LAC Δ psma β hld-pTX Δ α 1-4*), (Fig. 7B). For example, the cells exposed to PTX Δ 16 produce 85 \pm 10 pg/mL of IL-1 β 7 days post-infection. The level of IL-1 β was decreased to 40 \pm 5 pg/mL produced by the cells exposed to PTX Δ α β γ and was increased to 43 \pm 5 pg/mL, 70 \pm 10 pg/mL and 40 \pm 8 pg/mL

produced by the cells exposed to $LAC\Delta psma\beta hld$ -pTX $\Delta\alpha$ 1-4, $LAC\Delta psma\beta hld$ -pTX $\Delta\beta$ 1-2 and $LAC\Delta psma\beta hld$ -pTX Δhld correspondently.

To check if the difference in IL-1 β production was linked to the bacterial burden, we analyzed CFU numbers of tested strains. As shown in Fig 7C, there was no difference between the CFU numbers of all *S. aureus* strains used in our study 2 h post-infection. Six hours post-infection CFU of $LAC\Delta psma\beta hld$ -pTX $\Delta\alpha$ 1-4 was significantly higher than the CFU number of $LAC\Delta psma\beta hld$, while there were no differences between CFU numbers of $LAC\Delta psma\beta hld$ -pTX $\Delta\beta$ 1-2, $LAC\Delta psma\beta hld$ -pTX Δhld and $LAC\Delta psma\beta hld$, showing that the greater production of IL-1 β induced by $LAC\Delta psma\beta hld$ -pTX $\Delta\beta$ 1-2 strain did not depend on bacterial burden.

***S. aureus* clearance by osteoblasts-like MG-63 cells depends on caspase-1**

It has been reported that caspase-1 is essential for the restriction of intracellular pathogen replication in professional phagocytes (Amer *et al.*, 2006), however the role of caspase-1 in bacterial clearance in non-professional phagocytes, which include osteoblasts-like cells, has not been investigated. Here, we found that 6 h post infection the number of CFU was significantly higher in *CASP1*^{-/-}MG-63 cells than in WT MG-63 cells (Fig. 5). We therefore analyzed whether the lack of caspase-1 in *CASP1*^{-/-}MG-63 cells is correlated with a failure to control the intracellular replication of *S. aureus* bacteria. The quantity of intracellular bacteria during *S. aureus* infection of WT and *CASP1*^{-/-}MG-63 cells was determined after gentamicin treatment of infected cells. According to CFU determination bacterial internalization was not impaired in *CASP1*^{-/-}

Accepted Article

$^{-/-}$ MG-63 cells, as we observed equivalent levels of internalized bacteria in WT MG-63 cells 2 h post-infection, with $\sim 10^2$ CFU / 10^5 host cells. Six and 24 hours post-infection, the number of viable bacteria recovered from infected cells was significantly higher in *CASP1* $^{-/-}$ MG-63 than in WT MG-63 (Fig. 8A). These results suggest that the lack of caspase-1 impairs the ability of osteoblasts-like cells to restrict *S. aureus* growth. These findings were further confirmed using confocal microscopy. As shown in Fig. 8B, 6 h post-infection a considerably higher number of intracellular *S. aureus* cells (red) was observed in *CASP1* $^{-/-}$ MG-63 cells compared to WT MG-63 cells. This difference between the two cell types is even higher 24 h post infection. Phase contrast and fluorescent image of host cells bearing *S. aureus* were employed to visualize the intracellular localization of bacteria. We have presented inset boxes, which indicate the regions of the merged images that are shown at a higher magnification on the right of each image (Zoom) (Fig. 8B). As seen in Fig. 8B, mCherry expressing bacteria are localized in the host cell cytoplasm in the close vicinity to DAPI-stained nuclei. Three-dimension confocal microscopy was used to confirm the cytoplasmic localization of internalized *S. aureus*. Z-stack (Fig. 9A) was used to obtain 3D reconstituted images of *S. aureus*-infected host cells (Fig. 9B). Multiple images were acquired in different focal planes to create a Z-stack of images (data) through the Z axis. As seen in Fig. 9A, the sections close to the bottom of the slide culture chamber exhibited the blue fluorescence of the eukaryotic cells nuclei. Ascending within this “z-stack,” middle sections showed dots with intense red fluorescence, corresponding to internalized bacteria. The sections closed to the top of the slide culture chamber exhibited only blue

fluorescence of DAPI-stained nuclei, and red fluorescent bacteria was not detected anymore. Compartmentalisation of *S. aureus* inside WT MG-63 and *CASP1*^{-/-} MG-63 cells was examined by transmission EM. Phagosomal/lysosomal membranes were visible surrounding individual bacteria or clusters of bacteria (Fig. 9, C, red arrows) together with free bacterial cells in the cytosol (Fig. 9, C, black arrows).

Discussion

Despite antibiotic therapy and complex surgical procedures, *S. aureus* BJI is particularly difficult to treat. This is partly due to the tremendous capabilities of *S. aureus* to form biofilm, particularly in the presence of a foreign body as the formation of biofilm in the absence of material is not so frequently documented, and small-colony variants, and to invade and persist into osteoblasts, leading to chronicity and relapse of infection (Tuchscherer *et al.*, 2011; Vuong *et al.*, 2016; Trouillet-Assant *et al.*, 2016). To persist within the host cells, *S. aureus* also developed strategies to circumvent the host cell defenses (Alekseeva *et al.*, 2013; Deplanche *et al.*, 2015; Deplanche *et al.*, 2016; Deplanche *et al.*, 2019). Here we aimed to investigate the contributions of internalized *S. aureus* on alteration of host defense events such as inflammasomes activation and bacterial clearance in infected osteoblasts. The activation of inflammasomes during infection have been extensively characterized in professional phagocytes (Miller *et al.*, 2007; Lamkanfi and Dixit, 2009; Shimada *et al.*, 2010; Broz, 2016). The activation of inflammasomes was also demonstrated in infected osteoblasts, which play a key role in BJI (Yoshida *et al.*, 2017). Osteoblasts synthesize

various bone matrix proteins that are involved in bone formation, and that regulate the maturation of osteoclasts responsible for bone resorption (Ruscitti *et al.*, 2015). IL-1 β , a proinflammatory cytokine, plays a pivotal role in bone metabolism (Lee *et al.*, 2010). IL-1 β is mainly expressed by monocytes, macrophages, and dendritic cells (Lopez-Castejon and Brough, 2011; Franchi *et al.*, 2012; Lima-Junior *et al.*, 2013; Chang *et al.*, 2017), and is processed into a soluble mature form by active caspase-1, an inflammasomes compound. In the present work, we focused on the monitoring of soluble IL-1 β produced by infected osteoblasts. We employed an *in vitro* model of intracellular bacterial infection using human osteoblasts-like MG-63 cells infected with *S. aureus*.

We demonstrated that human osteoblast-like MG-63 cells release soluble IL-1 β 6 h post treatment with LPS+ATP, two inflammasome activators. IL-1 β release was concomittent with the appearance of an active caspase-1 20 kDa subunit, which results from an inflammasome activation in MG-63 cells. We noted that IL-1 β production in MG-63 cells started later and was much lower than IL-1 β production in THP-1 cells whose level of IL-1 β production was similar to those previously reported (Grahames *et al.*, 1999). Discrepancy in the levels of soluble IL-1 β released by MG-63 and THP-1 is likely related to their cell types. MG-63 are indeed non-professional phagocytes whereas PMA-treated THP-1 cells differentiate into macrophages and are professional phagocytes (Spano *et al.*, 2013).

We observed that an exposure of MG-63 cells to *S. aureus* results in the progressive increase in the level of IL-1 β . It started from a very low, but significant level, 6 h post-

infection to 100 pg/mL several days post-infection. This suggests that osteoblasts-like cells can play a role in the host defense mechanisms. Our findings corroborate clinical observations. Recent evaluation of the link between osteomyelitis, an inflammatory process usually associated with *S. aureus* infection and *IL1B* polymorphism, indeed indicates a potential involvement of the *IL1B*-511T allele, suggesting that disturbance of the IL-1 system is an important factor for osteomyelitis development (Alves De Souza *et al.*, 2017). A determination of IL-1 β concentration in the synovial fluids of spontaneously osteoarthritic porcine knees, provides a range of physiologic IL-1 β concentrations that can serve as a framework for the analysis of IL-1 β concentration in *in vitro* studies (McNulty *et al.*, 2013). Median IL-1 β concentration in synovial fluids was 0.109 ng/mL with mild osteoarthritis, which is similar to the IL-1 β concentrations found in our *in vitro* conditions.

Our results contrast with previous reports describing an increase in IL-1 β RNA expression but an absence of IL-1 β protein synthesis in 24 h infected mice osteoblasts (Marriott *et al.*, 2002). This discrepancy may result from the use of human MG-63 osteoblast-like cells in our work whereas mice primary cells were employed by Marriott and collaborators. Noteworthy, IL-1 β production by normal human osteoblasts-like cells was demonstrated 24 h after stimulation with LPS (Keeting *et al.*, 1991). The divergence between our results and the findings described by Marriott and collaborators may also result from the different *S. aureus* strains used in each study. We indeed showed that induction of IL-1 β release in infected cells is strongly strain-

dependent, with a 10-time lower IL-1 β production in cells infected with an Agr-deficient *S. aureus* strain.

Taking into account the pivotal role of caspase-1 in the maturation of IL-1 β , we generated a CASP1^{-/-}MG-63 cell line using CRISPR-Cas9 gene editing for the investigation of inflammasomes involvement during *S. aureus* infection in a model of BJI. Despite the fact that primary cells better resemble the natural state of the organism than immortalized cells, osteoblast-like MG-63 cells were employed for CRISPR-Cas9 gene editing because primary osteoblasts can only propagate for few generations *in vitro*, which is not enough for the establishment of a stable CASP1^{-/-}cell line. MG63 cells are cancer cells and are known to differ from primary osteoblasts, especially in phenotypes that may impact inflammasome activation. Our results show events upstream the caspase-1 maturation, such as NLRP3 expression and ASC specks formation, were observed equally in both WT MG-63 and CASP1^{-/-}MG-63 cells. Furthermore, we showed an absence of IL-1 β release following the stimulation with inflammasomes activators in CASP1^{-/-}MG-63 cells. We therefore consider that comparison of MG-63 cell line with CASP1^{-/-}MG-63 cells is relevant and the optimal model to investigate the role of inflammasomes and caspase-1 as well as pathogen clearance during infection.

The lack of IL-1 β production in infected CASP1^{-/-}MG-63 cells demonstrated a caspase-1 dependent mechanisms of IL-1 β production in human osteoblast-like cells. Our data corroborate observations of others who demonstrated caspase-1 dependent

mechanism of IL-1 β processing and release by mice macrophages during infection (Raupach *et al.*, 2006).

The absence of IL-1 β production by cells exposed to heat-killed bacteria indicates that factors associated with viable bacteria are involved in the activation of NLRP3 inflammasome. Employment of deletion and complemented PSMs mutants demonstrated that *S. aureus* toxins PSMs are involved in inflammasomes related IL-1 β production by infected osteoblast-like cells. We would like to highlight that IL-1 β production by infected osteoblasts appears to be particularly dependent on PSM β among PSMs. This is noteworthy, as no specific phenotypes has been attributed to those PSMs so far. It was shown previously that PSMs induce IL-1 β and IL-18 in human keratynocytes (Syed *et al.*, 2015). In the present work, we detected *S. aureus* in intracellular vesicles and in the cytosol of infected cells (see Fig. 4 for MW2 and Fig. 8 for SA113). It is generally accepted that the capacity to survive inside osteoblasts is due to the release of *S. aureus* from the vesicles to the cytoplasm that allows *S. aureus* escaping the proteolytic activity of the lysosome (Josse *et al.*, 2015). Giese *et al.* showed that PSM β rather than PSM α is responsible for the efficient escape of bacteria from phagosomes (Giese *et al.*, 2011). These latter observations suggest that after *S. aureus* internalization PSMs promote vacuolar rupture and induce the inflammasome activation resulting in the synthesis of inflammasome-associated protein such as IL-1 β in infected MG-63 cells. In addition to PSMs, the action of other factors cannot be excluded since complemented mutants did not entirely restore the level of secreted IL-1 β .

The role of caspase-1 in the production of inflammatory cytokines has been extensively investigated (Franchi *et al.*, 2012; Sollberger *et al.*, 2014), while much less attention has been paid to its impact on other immune processes. Nevertheless, many investigations point out that in addition to the processing of IL-1 β and IL-18, caspase-1 regulates unconventional protein secretion (Keller *et al.*, 2008), activates lipid metabolic pathway (Gurcel *et al.*, 2006), restricts pathogens replication in professional phagocytes (Master *et al.*, 2008; Akhter *et al.*, 2009) and induces pyroptosis, a proinflammatory cell death (Fernandes-Alnemri *et al.*, 2007).

Our investigation of host defense event during *S. aureus* infection of non-professional phagocytes, such as the control of intracellular bacterial proliferation, reveals a drastic increase in the proliferation of internalized bacteria in osteoblastic CASP1^{-/-}MG-63 cells. This finding is in keeping with the previous reports demonstrating the correlation of the lack of caspase-1 activation with a failure to restrict the replication of *S. aureus* inside phagocytic cells (Sokolovska *et al.*, 2013; Cohen *et al.*, 2018). Indeed, it has been demonstrated that, during *S. aureus* infection of professional phagocytes NLRP3, inflammasomes and caspase-1 regulate phagosomes acidification that is essential for the activation of the hydrolytic enzymes required for the killing of internalized bacteria (Ip *et al.*, 2010; Sokolovska *et al.*, 2013). Moreover, it was suggested that early activation of NLRP3 (Ip *et al.*, 2010; Sokolovska *et al.*, 2013) inflammasomes is triggered by events, such as the production of ROS, that are associated with the phagocytic process in macrophages (Sokolovska *et al.*, 2013). Recently, we demonstrated that *S. aureus* induces the production of ROS in WT MG-63 cells

(Deplanche *et al.*, 2019). We hypothesize that *S. aureus*-induced ROS plays a similar role in inflammasome activation in non-phagocytic cells.

Collectively, our results demonstrate that human osteoblast-like MG-63 cells induce an immune response against *S. aureus* through inflammasomes activation and processing of IL-1 β , the master cytokine of inflammation (Dinarello *et al.*, 2012). The outcome of the infection depends on the balance between the host immune response and the action of main *S. aureus* virulence factors, such as PSMs, whose production may differ among the *S. aureus* strains, as we have already observed in our previous work (Deplanche *et al.*, 2015). Besides our observations of inflammasomes activation, we demonstrated that CASP1^{-/-}MG-63 cells were unable to restrict the intracellular replication of *S. aureus*. It points out that the active caspase-1 prevents exacerbated intracellular replication of *S. aureus* in non-professional phagocytes in addition to professional phagocytes, suggesting the pivotal role of caspase-1 in *S. aureus* clearance independently from the type of cells. Considering this latter point, it would be interesting to estimate the possible role of different PSMs using various *S. aureus* wild type and PSMs mutants in the activation of Caspase-1 during long-term infection of osteoblasts. Our findings deserve further investigation to elucidate whether caspase-1 is involved in the clearance of other pathogens. Our results raise the fascinating possibility, that pathogens, which inhibit caspase-1 activation, do so not only to govern the generation of inflammatory cytokines but also to permit bacterial replication in infected cells. Current findings redefine our understanding of the role of

osteoblasts in BJI, suggesting that osteoblasts, are not passive bystanders, but active players in host defenses against *S. aureus* infection.

Experimental procedures

Selection of the cell model.

Based on protein sequence human caspase-4 and -5 are considered as the inflammasome-associated caspases most homologous to mice caspase-11, however there is a some difference in their mechanism activation (Viganò *et al.*, 2015). Consequently, in order to study the inflammasomes activation during *S. aureus* infection in the context of BJI in human we opted for the human cells.

To silence the selected gene one can use RNA interference or the CRISPR-Cas9 gene editing approach (Québatte and Dehio, 2017). Since the RNAi-mediated knockdown of expression often is not complete, the CRISPR-Cas9 editing approach was selected. Despite the fact that primary cells better reassemble the natural state of the organism than immortalized cells, osteoblast-like MG-63 cells were selected for CRISPR-Cas9 gene editing. Primary cells have a limited life span in cell culture experiments that is not sufficient for the establishment of a stable gene-deficient cell line. Moreover, freshly isolated primary cells may still have an innate mechanism to resist foreign genetic material resulting in the degradation of CRISPR components. Taking into account those points we are convinced that at present the CRISPR-Cas9 editing approach using osteoblast-like cells is the appropriate model to study the role of caspase-1 in inflammasomes activation in the context of BJI.

Maintenance of eukaryotic cells lines. The human osteoblast-like MG-63 (LGC Standards, Teddington, UK) cells and human monocyte THP1 cells (ATCC TIB-202) were cultured in DMEM and RPMI 1640 respectively, supplemented with 10% fetal calf serum (Gibco), 100 U/mL penicillin, and 100 µg/mL streptomycin at 37°C with 5% CO₂ as described (Deplanche *et al.*, 2019). Trypsin/EDTA (Sigma) was used for cell subculturing to release adherent cells. In order to differentiate THP1 cells into macrophages, cells were treated with 20 nM phorbol 12-myristate 13-acetate (PMA) for 48 h (Richter *et al.*, 2016).

Depletion of caspase-1 in human osteoblasts-like MG-63 using the CRISPR-Cas9 gene editing system. The caspase-1 gene editing in MG-63 cells was performed using CRISPR-Cas9 technology (Mali *et al.*, 2013). The sgRNA sequence (ATTGACTCCGTTATTCCGAA), which as previously published targets the *CASP1* gene (Schmid-Burgk *et al.*, 2015), was cloned into the lentiCRISPR v2 (Addgene #52961) (Sanjana *et al.*, 2014). Gene editing was achieved *via* lentiviral infection of MG-63 cells. Lentiviral production has been performed as recommended (<http://tronolab.epfl.ch>) and previously described (Gilot *et al.*, 2017). After antibiotic selection [puromycine (3 days, 1µg/mL)], cells were seeded in 96-well plates at 0.3 cells/well for single cell clonal expansion. Single-cell clones were tested by Western blot analysis for the presence of the 45 kDa band corresponding to pro-caspase-1. Six clones that did not present 45-kDa bands were recloned in 96-well plates (10 and 30 cells per plate). Afterwards, single-cell clones were transferred in 6-wells plate and

grown to 80% of confluence. Three clones originating from three different parental clones that lacked 45-kD bands (Western Blot) were recloned in 96-well plates (10 and 30 cells per plate). All monoclonal lines lacked 45-kD bands (Western blot). Again, three clones originated from three different parental clones were selected and grown in 25-mL flasks. CRISPR-induced genomic modifications were verified by nucleotide sequence analysis, and the lack of caspase-1 was confirmed by Western blot analysis.

S. aureus strain description. The methicillin-resistant strains *S. aureus* MW2 (USA400), LAC (USA300) wild type, the isogenic mutant LAC $\Delta psm\alpha\beta hld$, which lacks the *psm\alpha* and *psm\beta* operons and in which translation of the *hld* gene is abolished by mutation of the start codon, LAC (pTX Δ 16) which carries the control plasmid, the deletion mutant LAC $\Delta psm\alpha\beta hld$ (pTX Δ 16) and the complemented strains expressing either the four PSM α peptides (LAC $\Delta psm\alpha\beta hld$ -pTX $\Delta\alpha$ 1-4), the two PSM β peptides (LAC $\Delta psm\alpha\beta hld$ -pTX $\Delta\beta$ 1-2), or the δ -toxin (LAC $\Delta psm\alpha\beta hld$ -pTX Δhld) were obtained from the Laboratory of Bacteriology, NIH, USA (Wang *et al.*, 2007; Joo and Otto, 2014). The pTX Δ 16 plasmids were derived from plasmid pTX15 with the deletion of the *xyIR* repressor gene. The tetracycline-resistant strains harboring plasmid pTX Δ 16 were grown in BHI containing 12.5 μ g/mL of tetracycline. *S. aureus* SA113, which is an agr-deficient derivative of *S. aureus* strain NCTC8325 (Iordanescu and Surdeanu, 1976), and SA113 (pctuf-mCherry) strain, which carries a plasmid encoding mCherry (red fluorescence) fused with the propeptide of lipase for fluorescence enhancement, were obtained from the Laboratory of Microbial Genetics, University of Tübingen

(Mauthe *et al.*, 2012). Aliquots from overnight cultures on BHI broth were diluted (1:50) in DMEM. The growth curves of mutants were similar to that of the wild type. Strains were grown at 37°C under anaerobic conditions until cultures reached an optical density of 0.6 at 600 nm, corresponding to 10⁸ CFU/mL (Colony Forming Units). CFU were determined after plating a bacterial suspension on BHI agar followed by overnight incubation as described (Alekseeva *et al.*, 2013).

Cell culture infection. 2.5x10⁵ of either MG-63, *CASP1*^{-/-}MG-63, or THP1 cells were seeded in the wells of 12-well plates. Experiments were performed with PMA-treated THP1 cells. Cells then were exposed to *S. aureus* strains at MOI 50:1. An MOI value of 50:1 was selected in order to prevent the induction of host cell death (Deplanche *et al.*, 2019). Bacterial concentrations were estimated spectrophotometrically and were confirmed by determination of CFU. Extracellular bacteria were removed 2 h post-infection by incubating cells in cDMEM with 20 µg/mL lysostaphin and 100 µg/mL gentamicin for 2 h, which eliminates extracellular bacteria without altering intracellular bacteria (Alekseeva *et al.*, 2013; Deplanche *et al.*, 2015), followed by incubation in cDMEM containing 25 µg/mL of gentamicin. After the indicated periods adherent and floating cells were collected, centrifuged, and prepared either for Western blot analysis or for analysis by cytofluorometry.

For the determination of the number of internalized bacteria, we used the method we have previously described (Bouchard *et al.*, 2013; Alekseeva *et al.*, 2013) Briefly, to determine the number of internalized bacteria after 2 h of infection, infected cells were

lysed with 0.05% Triton X-100 in PBS, cell lysates were plated on BHI agar at different dilutions, and CFU were determined after overnight incubation as described (Bouchard *et al.*, 2013; Alekseeva *et al.*, 2013).

To determine the intracellular survival rate of internalized *S. aureus* SA113 the initial internalized bacterial population was measured 2 h post-infection and was used as the starting point for intracellular survival assay and was considered as 100%. The internalized *S. aureus* SA113 population at the different periods was measured and expressed relative to an *S. aureus* SA113 initial internalization (2 h post-infection).

Gene expression analysis by qRT-PCR

Human WT MG-63 and *CASP1*^{-/-}MG-63 G2 cells were exposed to inducers of inflammasomes activation, 5 mM ATP for 30 min, following by the exposure to 5 mg/mL nigericin for 3 h. Relative NLRP3 mRNA expression was evaluated by quantitative Real-Time PCR (qRT-PCR), as described (Deplanche *et al.*, 2015). Briefly, the total RNA was isolated with a RNA II kit (Macherey Nagel) and the cDNA was synthesized using a qScript cDNA Synthesis kit (Quanta Biosciences). Reactions devoid of reverse transcriptase and reactions containing H₂O instead of cDNA were used as negative controls. Primers for human NLRP3 were designed according to the sequences available at the National Center Biotechnology Information <http://www.ncbi.nlm.nih.gov/> (NLRP3, NCBI accession number NM_001079821.2), 5'-GAAGCACCTGTTGTGCAATC-3', 5'-GCAAGATCCTGACAACATGC-3'.

Glyceraldehyde-3-phosphate dehydrogenase (GAPDH, NCBI accession # NM2046.3) f5'-CAAGGGCATCCTGGGCTAC-3', r5'-GGTGGTCCAGGGGTCTTACT-3' and PeptidylProyl Isomérase A (PPIA, NCBI accession #NM_001300981) f5'-GACCCAACACAAATGGTTCC-3', r5'-TCGAGTTGTCCACAGTCAGC-3' were used as housekeeping genes. Relative quantification relates the PCR signal of the target transcript in a treatment group to that of an untreated control. Each 13 µl PCR mixture included 2 µl of cDNA, 200 nM of primers, 12.5 µl of IQ Sybr Green supermix (2x) (Biorad) and H₂O. Amplification was carried out on a CFX96 Real Time System (BioRad, Marne la Coquette, France) for 3 min at 95°C and 40 cycles of two steps consisting of 5 s at 95°C and 30 s at 60°C. The relative quantification of the mRNA levels of the target genes was determined using CFX Manager based on the deltaCT –method (Livak and Schmittgen, 2001). The amount of target was normalized to PPIA and GAPDH genes: $\text{deltaCT} = \text{CT} (\text{target gene}) - \text{CT} (\text{housekeeping gene})$ where CT represents the cycle number required to reach a defined threshold target abundance. The relative mRNA level was calculated as x^{deltaCT} ($x = \text{Primer efficiency}$). After normalization relative quantification refers to the PCR signal of the target transcript in a treatment group divided by the values obtained from control cells arbitrarily set to 1 at the indicated period.

Transmission electron microscopy (Transmission EM). MG-63 cells were fixed in 2.5% glutaraldehyde/cacodylate buffer; then in 1% osmium tetroxide. The pellet was mixed with 3% agar in sodium cacodylate, 7,3 dehydrated, embedded in Epon-

Araldite-DMP30 resin mixture and polymerized at 60°C for 48 h. Sections were cut in Leica ultra microtome, stained with uranyl acetate and were analyzed with JEOL 1400 Electron Microscope (Jeol, Tokyo, Japan). Images were digitally captured with GATAN Orius camera (Digital Micrograph Software).

Western blot analysis. Pro-caspase-1 and cleaved caspase-1 were detected by Western blot analysis as described (Berkova *et al.*, 2006). Briefly, 2.5×10^5 of cells were grown in 12-well plates. Pro-caspase-1 was detected in non-stimulated and stimulated cells, while active caspase-1 was detected solely in stimulated cells. Wild type (WT) MG-63 or *CASP1*^{-/-} MG-63 cells were primed for 3 h with LPS (1 µg/mL) (Sigma) and selected samples were stimulated with ATP (5 mM) for 15 min or after the exposure to *S. aureus* strains. Six hours after the beginning of the treatment cells together with cell-culture supernatants were collected and diluted in RIPA lysis buffer supplemented with complete protease inhibitor cocktail, P8340 (Sigma Aldrich®). Protein samples were prepared in 5x polyacrylamide gel electrophoresis (SDS-PAGE) sample loading buffer. Proteins were separated on 12% SDS-PAGE gels and transferred onto 0.2 µM PVDF membranes. The membranes were washed three times in PBS-T (Tris-buffered saline containing 0.5% Tween 20) and blocked in 10% skim milk in PSB-T for 1 h at room temperature before being incubated with primary antibody overnight at 4°C. Caspase-1 was detected with anti-human caspase-1 antibody (1:1,000 dilution, mAb p/20, AdipoGen). Membranes were washed four times in PBS-T and incubated with HRP-conjugated secondary anti-mouse IgG-HRP antibody 1:10,000 dilution, Cell Signaling

Ozyme) for 1 h at room temperature, washed another four times, and incubated with Western chemiluminescent HRP substrate (ECL kit) (GE Healthcare). The image was processed using a GBOX imaging system (Syngene, Ozyme, Poitiers, France). To assess the quantity of loaded protein, membranes were re-probed with rabbit anti-tubuline (Cell Signaling Ozyme France) (1:1000) and bands were visualized using the ECL kit and a GBOX imaging system.

Flow cytometry analysis. For an estimation of NLRP3 protein expression in WT MG-63 vs CASP1^{-/-} MG-63 cells, cells were exposed to *S. aureus* LAC for 2 h and were fixed in 4% paraformaldehyde/PBS followed by permeabilization in 0.1% Triton/0.5% BSA/PBS. After centrifugation, cells were resuspended in 200 µl of 0.5% BSA/PBS, 5 µl of Rat Anti-Human NLRP3 Alexa Fluor® 488-conjugated Monoclonal Antibody (Catalog # IC7578G) or isotype control antibody (Catalog # IC006G) per 10⁶ cells were added, and the samples were incubated for 45 min. NLRP3 expression was analyzed with an Accuri C6 flow cytometer. Data were collected from 20,000 cells, and analyzed with CFlow software (Becton Dickinson) as described (Nguyen *et al.*, 2016).

Confocal microscopy. WT MG-63 or CASP1^{-/-}MG-63 cells were grown on cover slips and exposed to *S. aureus* SA113 (MOI 50:1) for 2 h. Six and 24 h post-infection, cells were fixed with 4% paraformaldehyde/PBS for 20 min, followed by permeabilisation in 0.1% triton/PBS and incubation with 20% goat serum (Sigma) as described (Deplanche *et al.*, 2019). Rabbit anti-PYCARD antibody (Coger France) diluted 1:50 in

1% BSA/PBS was applied overnight at 4°C, followed by incubation with Alexa Fluor 488 labeled goat anti-rabbit antibody (Cell Signaling Ozyme) (1:1000) for 2 h. Cover slips were mounted with ProLong antifade containing DAPI (Vectashield, Biovalley).

Confocal laser scanning microscopy (CLSM) observation of specimens was performed using a ZEISS LSM 880 inverted confocal microscope (Carl Zeiss AG, Oberkochen, Germany) equipped with immersion objective 63× (Plan Apochromat objective, oil immersion, NA 1.4) driven by Zen software. The pinhole is set to the one Airy unit.

To quantify the amount of ASC-speck forming cells the number of ASC speck out of 100 cells in the culture of WT MG-63 cells vs *CASP1*^{-/-} MG-63, G2, B9 and C2 clones was enumerated.

To obtain three dimensional images of host cells infected by *S. aureus* multiple images were acquired in different focal planes to create a Z-stack of images (data) through the Z axis.

IL-1 beta quantification by ELISA. WT MG-63, *CASP1*^{-/-}MG-63 or THP1 cells were exposed either to inflammasomes inducers 1 mg/mL LPS for 30 min followed by the exposure to 5 mM ATP for 15 min (LPS+ATP) or to *S. aureus* strains. Undiluted cell culture supernatants were subjected to human IL-1β detection by sandwich-ELISA (Thermofischer Life Technologies, INVITROGEN 88-7261) according to the manufacturer's instructions. Briefly, wells of 96-wells plates were coated with capture anti-human IL-1β antibody and were incubated overnight at 4°C. After washing the wells were incubated in the blocking solution. Then tested samples were added to the

appropriate wells. A standard curve was measured with 2-fold serial dilutions of the maximal standard concentration of 150 pg/mL. Recombinant human IL-1 β was used for generating the standard curve and calibrating samples. After 2 h of incubation, biotin-conjugated anti-human IL-1 β antibody was added to the wells followed by incubation with avidin-HRP for 30 min. After addition of the tetramethylbenzidine substrate solution for 15 min the reaction was stopped with stop solution and absorbance was read at 450 nm. The sensitivity of IL-1 β detection is 2 pg/mL.

Statistical analysis

At least three independent assays were performed per experiment. The differences among the groups were assessed by analysis of variance (ANOVA). P-values < 0.05 were considered to be significant. Tukey's Honestly Significant Difference test was applied for comparison of means between the groups. The values are expressed as mean \pm standard deviation (\pm SD).

Author's Contributions

M.O, Y.L.L and N.B. designed the study. E.L.L., A.G., M.D., J.O., M.T.N. and F.L.R.C. performed the experiments. A.G., N.B., D.G. and A.N. selected CRISPR sgRNA, E.L.L., A.G. and N.B. performed experiments related to CRISPR gene editing. M.O., V.A., E.L.L., Y.L.L, F.G. and N.B. analyzed the results. M.O., Y.L.L., E.L.L. and N.B. wrote the manuscript.

All authors reviewed the Manuscript.

Acknowledgments

The authors thank Pr. Petr Broz, Department of Biochemistry, University of Lausanne, Epalinges, Switzerland for his help in design of experiments related to CRISPR editing, for invaluable suggestions in the analysis of results, for discussion and corrections of the manuscript. We thank Mary Bret for the English corrections. We thank Chantal Cauty (STLO) and Agnes Burel (MRic, Rennes University) for their precious help in performing Transmission EM.

The program Germaine de Stael, PHC bi-lateral France–Switzerland collaboration (to N.B. and P.B.), French National Institute for Agricultural Research (INRA), Metaprogram GISA, LONGhealth - MPP10573 (to N.B. and M.D), the Intramural Research Program of the National Institute of Allergy and Infectious Diseases (NIAID), U.S. National Institutes of Health (NIH), project number 1 ZIA AI000904 (to M.O.), the Deutsche Forschungsgemeinschaft (DFG) SFB766 (to F.G. and M.T). E. L. L. is a recipient of a Ph.D. fellowship from Coordenação de Aperfeiçoamento de Pessoal de Nível Superior (CAPES; Brazil). The ZEISS LSM880 confocal microscope was funded by the European Union (FEDER), the French Ministry of Education, Research and Innovation, the Regional Council of Brittany and INRA.

Author's contribution

Conflict of Interest

The authors declare no competing financial and/or non-financial interests, all authors concur with the submission

References

- Akhter, A., Gavrilin, M.A., Frantz, L., Washington, S., Ditty, C., Limoli, D., *et al.* (2009) Caspase-7 activation by the Nlrc4/Ipaf inflammasome restricts Legionella pneumophila infection. *PLoS Pathog* **5**: e1000361.
- Alekseeva, L., Rault, L., Almeida, S., Legembre, P., Edmond, V., Azevedo, V., *et al.* (2013) *Staphylococcus aureus*-induced G2/M phase transition delay in host epithelial cells increases bacterial infective efficiency. *PLoS One* **8** <https://www.ncbi.nlm.nih.gov/pmc/articles/PMC3662696/>. Accessed February 20, 2018.
- Alves De Souza, C., Queiroz Alves De Souza, A., Queiroz Alves De Souza, M. do S., Dias Leite, J.A., Silva De Moraes, M., and Baresch Rabenhorst, S.H. (2017) A link between osteomyelitis and IL1RN and IL1B polymorphisms—a study in patients from Northeast Brazil. *Acta Orthop* **88**: 556–561.
- Amer, A., Franchi, L., Kanneganti, T.-D., Body-Malapel, M., Ozören, N., Brady, G., *et al.* (2006) Regulation of Legionella phagosome maturation and infection through flagellin and host Ipaf. *J Biol Chem* **281**: 35217–35223.
- Berkova, N., Lair-Fullerger, S., Féménia, F., Huet, D., Wagner, M.-C., Gorna, K., *et al.* (2006) *Aspergillus fumigatus* conidia inhibit tumour necrosis factor- or staurosporine-induced apoptosis in epithelial cells. *Int Immunol* **18**: 139–150.
- Bouchard, D.S., Rault, L., Berkova, N., Le Loir, Y., and Even, S. (2013) Inhibition of *Staphylococcus aureus* invasion into bovine mammary epithelial cells by contact with live Lactobacillus casei. *Appl Environ Microbiol* **79**: 877–885.
- Broz, P. (2016) Inflammasomes: intracellular detection of extracellular bacteria. *Cell Res* **26**: 859–860.
- Broz, P., and Dixit, V.M. (2016) Inflammasomes: mechanism of assembly, regulation and signalling. *Nat Rev Immunol* **16**: 407–420.
- Chang, T.-H., Huang, J.-H., Lin, H.-C., Chen, W.-Y., Lee, Y.-H., Hsu, L.-C., *et al.* (2017) Dectin-2 is a primary receptor for NLRP3 inflammasome activation in dendritic cell response to Histoplasma capsulatum. *PLoS Pathog* **13**: e1006485.
- Choi, Y.J., Kim, S., Choi, Y., Nielsen, T.B., Yan, J., Lu, A., *et al.* (2019) SERPINB1-mediated checkpoint of inflammatory caspase activation. *Nat Immunol* **20**: 276–287.

Cohen, T.S., Boland, M.L., Boland, B.B., Takahashi, V., Tovchigrechko, A., Lee, Y., *et al.* (2018) *S. aureus* evades macrophage killing through NLRP3-dependent effects on mitochondrial trafficking. *Cell Rep* **22**: 2431–2441.

Del Pozo, J.L., and Patel, R. (2009) Infection associated with prosthetic Joints. *N Engl J Med* **361**: 787–794.

Deplanche, M., Alekseeva, L., Semenovskaya, K., Fu, C.-L., Dessauge, F., Finot, L., *et al.* (2016) Staphylococcus aureus Phenol-Soluble Modulins Impair Interleukin Expression in Bovine Mammary Epithelial Cells. *Infect Immun* **84**: 1682–1692.

Deplanche, M., Filho, R.A.E.-A., Alekseeva, L., Ladier, E., Jardin, J., Henry, G., *et al.* (2015) Phenol-soluble modulin α induces G2/M phase transition delay in eukaryotic HeLa cells. *FASEB J* **29**: 1950–1959.

Deplanche, M., Mouhali, N., Nguyen, M.-T., Cauty, C., Ezan, F., Diot, A., *et al.* (2019) *Staphylococcus aureus* induces DNA damage in host cell. *Sci Rep* **9**: 7694.

Dinarello, C.A., Simon, A., and Meer, J.W.M. van der (2012) Treating inflammation by blocking interleukin-1 in a broad spectrum of diseases. *Nat Rev Drug Discov* **11**: 633–652.

Feng, Q., Li, P., Leung, P.C.K., and Auersperg, N. (2004) Caspase-1zeta, a new splice variant of the caspase-1 gene. *Genomics* **84**: 587–591.

Fernandes-Alnemri, T., Wu, J., Yu, J.-W., Datta, P., Miller, B., Jankowski, W., *et al.* (2007) The pyroptosome: a supramolecular assembly of ASC dimers mediating inflammatory cell death via caspase-1 activation. *Cell Death Differ* **14**: 1590–1604.

Flannagan, R.S., Heit, B., and Heinrichs, D.E. (2016) Intracellular replication of *Staphylococcus aureus* in mature phagolysosomes in macrophages precedes host cell death, and bacterial escape and dissemination. *Cell Microbiol* **18**: 514–535.

Franchi, L., Kamada, N., Nakamura, Y., Burberry, A., Kuffa, P., Suzuki, S., *et al.* (2012) NLR4-driven production of IL-1 β discriminates between pathogenic and commensal bacteria and promotes host intestinal defense. *Nat Immunol* **13**: 449–456.

Giese, B., Glowinski, F., Paprotka, K., Dittmann, S., Steiner, T., Sinha, B., and Fraunholz, M.J. (2011) Expression of δ -toxin by *Staphylococcus aureus* mediates escape from phago-endosomes of human epithelial and endothelial cells in the presence of β -toxin. *Cellular Microbiology* **13**: 316–329.

Gilot, D., Migault, M., Bachelot, L., Journé, F., Rogiers, A., Donnou-Fournet, E., *et al.* (2017) A non-coding function of TYRP1 mRNA promotes melanoma growth. *Nat Cell Biol* **19**: 1348–1357.

Grahames, C.B., Michel, A.D., Chessell, I.P., and Humphrey, P.P. (1999) Pharmacological characterization of ATP- and LPS-induced IL-1 β release in human monocytes. *Br J Pharmacol* **127**: 1915–1921.

Gurcel, L., Abrami, L., Girardin, S., Tschopp, J., and Goot, F.G. van der (2006) Caspase-1 activation of lipid metabolic pathways in response to bacterial pore-forming toxins promotes cell survival. *Cell* **126**: 1135–1145.

Herbert, S., Ziebandt, A.-K., Ohlsen, K., Schäfer, T., Hecker, M., Albrecht, D., *et al.* (2010) Repair of global regulators in *Staphylococcus aureus* 8325 and comparative analysis with other clinical isolates. *Infect Immun* **78**: 2877–2889.

Higa, N., Toma, C., Nohara, T., Nakasone, N., Takaesu, G., and Suzuki, T. (2013) Lose the battle to win the war: bacterial strategies for evading host inflammasome activation. *Trends Microbiol* **21**: 342–349.

Iordanescu, S., and Surdeanu, M. (1976) Two restriction and modification systems in *Staphylococcus aureus* NCTC8325. *J Gen Microbiol* **96**: 277–281.

Ip, W.K.E., Sokolovska, A., Charriere, G.M., Boyer, L., Dejardin, S., Cappillino, M.P., *et al.* (2010) Phagocytosis and phagosome acidification are required for pathogen processing and MyD88-dependent responses to *Staphylococcus aureus*. *J Immunol* **184**: 7071–7081.

Joo, H.-S., and Otto, M. (2014) The isolation and analysis of phenol-soluble modulins of *Staphylococcus epidermidis*. *Methods Mol Biol* **1106**: 93–100.

Josse, J., Velard, F., and Gangloff, S.C. (2015) *Staphylococcus aureus* vs. Osteoblast: Relationship and Consequences in Osteomyelitis. *Front Cell Infect Microbiol* **5**
<https://www.ncbi.nlm.nih.gov/pmc/articles/PMC4660271/>. Accessed February 27, 2018.

Kahl, B.C., Becker, K., and Löffler, B. (2016) Clinical Significance and Pathogenesis of Staphylococcal Small Colony Variants in Persistent Infections. *Clin Microbiol Rev* **29**: 401–427.

Kazemzadeh-Narbat, M., Noordin, S., Masri, B.A., Garbuz, D.S., Duncan, C.P., Hancock, R.E.W., and Wang, R. (2012) Drug release and bone growth studies of antimicrobial peptide-loaded calcium phosphate coating on titanium. *J Biomed Mater Res Part B Appl Biomater* **100**: 1344–1352.

Keeting, P.E., Rifas, L., Harris, S.A., Colvard, D.S., Spelsberg, T.C., Peck, W.A., and Riggs, B.L. (1991) Evidence for interleukin-1 beta production by cultured normal human osteoblast-like cells. *J Bone Miner Res* **6**: 827–833.

Keller, M., Rüegg, A., Werner, S., and Beer, H.-D. (2008) Active caspase-1 is a regulator of unconventional protein secretion. *Cell* **132**: 818–831.

Koh, E.T., Torabinejad, M., Pitt Ford, T.R., Brady, K., and McDonald, F. (1997) Mineral trioxide aggregate stimulates a biological response in human osteoblasts. *J Biomed Mater Res* **37**: 432–439.

Kremserova, S., and Nauseef, W.M. (2019) Frontline Science: *Staphylococcus aureus* promotes receptor-interacting protein kinase 3- and protease-dependent production of IL-1 β in human neutrophils. *J Leukoc Biol* **105**: 437–447.

Lamkanfi, M., and Dixit, V.M. (2009) The Inflammasomes. *PLOS Pathogens* **5**: e1000510.

Lamkanfi, M., and Dixit, V.M. (2014) Mechanisms and functions of inflammasomes. *Cell* **157**: 1013–1022.

Lee, Y.-M., Fujikado, N., Manaka, H., Yasuda, H., and Iwakura, Y. (2010) IL-1 plays an important role in the bone metabolism under physiological conditions. *Int Immunol* **22**: 805–816.

Lima-Junior, D.S., Costa, D.L., Carregaro, V., Cunha, L.D., Silva, A.L.N., Mineo, T.W.P., *et al.* (2013) Inflammasome-derived IL-1 β production induces nitric oxide-mediated resistance to Leishmania. *Nat Med* **19**: 909–915.

Liu, G.Y. (2009) Molecular pathogenesis of *Staphylococcus aureus* infection. *Pediatr Res* **65**: 71R-77R.

Livak, K.J., and Schmittgen, T.D. (2001) Analysis of relative gene expression data using real-time quantitative PCR and the 2(-Delta Delta C(T)) Method. *Methods* **25**: 402–408.

Lopez-Castejon, G., and Brough, D. (2011) Understanding the mechanism of IL-1 β secretion. *Cytokine Growth Factor Rev* **22**: 189–195.

Ma, M., Pei, Y., Wang, X., Feng, J., Zhang, Y., and Gao, M.-Q. (2019) LncRNA XIST mediates bovine mammary epithelial cell inflammatory response via NF- κ B/NLRP3 inflammasome pathway. *Cell Prolif* **52**: e12525.

Mali, P., Yang, L., Esvelt, K.M., Aach, J., Guell, M., DiCarlo, J.E., *et al.* (2013) RNA-guided human genome engineering via Cas9. *Science* **339**: 823–826.

Maltez, V.I., Tubbs, A.L., Cook, K.D., Achoui, Y., Falcone, E.L., Holland, S.M., *et al.* (2015) Inflammasomes coordinate pyroptosis and natural killer cell cytotoxicity to clear infection by a ubiquitous environmental bacterium. *Immunity* **43**: 987–997.

Mariathasan, S., Newton, K., Monack, D.M., Vucic, D., French, D.M., Lee, W.P., *et al.* (2004) Differential activation of the inflammasome by caspase-1 adaptors ASC and Ipaf. *Nature* **430**: 213–218.

Marriott, I., Hughes, F.M., and Bost, K.L. (2002) Bacterial infection of osteoblasts induces interleukin-1 β and interleukin-18 transcription but not protein synthesis. *J Interferon Cytokine Res* **22**: 1049–1055.

Master, S.S., Rampini, S.K., Davis, A.S., Keller, C., Ehlers, S., Springer, B., *et al.* (2008) *Mycobacterium tuberculosis* prevents inflammasome activation. *Cell Host Microbe* **3**: 224–232.

Masumoto, J., Taniguchi, S., and Sagara, J. (2001) Pyrin N-terminal homology domain- and caspase recruitment domain-dependent oligomerization of ASC. *Biochem Biophys Res Commun* **280**: 652–655.

Mauthe, M., Yu, W., Krut, O., Krönke, M., Götz, F., Robenek, H., and Proikas-Cezanne, T. (2012) WIPI-1 positive autophagosome-like vesicles entrap pathogenic *Staphylococcus aureus* for lysosomal degradation. *Int J Cell Biol* **2012**: 179207.

McGilligan, V.E., Gregory-Ksander, M.S., Li, D., Moore, J.E., Hodges, R.R., Gilmore, M.S., *et al.* (2013) *Staphylococcus aureus* activates the NLRP3 inflammasome in human and rat conjunctival goblet cells. *PLoS ONE* **8**: e74010.

McNulty, A.L., Rothfus, N.E., Leddy, H.A., and Guilak, F. (2013) Synovial fluid concentrations and relative potency of interleukin-1 alpha and beta in cartilage and meniscus degradation. *J Orthop Res* **31**: 1039–1045.

Miller, L.S., Pietras, E.M., Uricchio, L.H., Hirano, K., Rao, S., Lin, H., *et al.* (2007) Inflammasome-mediated production of IL-1beta is required for neutrophil recruitment against *Staphylococcus aureus* in vivo. *J Immunol* **179**: 6933–6942.

Mohamed, W., Sommer, U., Sethi, S., Domann, E., Thormann, U., Schütz, I., *et al.* (2014) Intracellular proliferation of *S. aureus* in osteoblasts and effects of rifampicin and gentamicin on *S. aureus* intracellular proliferation and survival. *Eur Cell Mater* **28**: 258–268.

Morales, A.J., Carrero, J.A., Hung, P.J., Tubbs, A.T., Andrews, J.M., Edelson, B.T., *et al.* (2017) A type I IFN-dependent DNA damage response regulates the genetic program and inflammasome activation in macrophages. *Elife* **6**.

Nguyen, M.-T., Deplanche, M., Nega, M., Le Loir, Y., Peisl, L., Götz, F., and Berkova, N. (2016) *Staphylococcus aureus* Lpl lipoproteins delay G2/M phase transition in HeLa cells. *Front Cell Infect Microbiol* **6** <https://www.ncbi.nlm.nih.gov/pmc/articles/PMC5187369/>. Accessed February 20, 2018.

Otto, M. (2010) Basis of virulence in community-associated methicillin-resistant *Staphylococcus aureus*. *Annu Rev Microbiol* **64**: 143–162.

Periasamy, S., Joo, H.-S., Duong, A.C., Bach, T.-H.L., Tan, V.Y., Chatterjee, S.S., *et al.* (2012) How *Staphylococcus aureus* biofilms develop their characteristic structure. *Proc Natl Acad Sci USA* **109**: 1281–1286.

Québatte, M., and Dehio, C. (2017) Systems-level interference strategies to decipher host factors involved in bacterial pathogen interaction: from RNAi to CRISPRi. *Curr Opin Microbiol* **39**: 34–41.

Queck, S.Y., Jameson-Lee, M., Villaruz, A.E., Bach, T.-H.L., Khan, B.A., Sturdevant, D.E., *et al.* (2008) RNAIII-independent target gene control by the agr quorum-sensing system: insight into the evolution of virulence regulation in *Staphylococcus aureus*. *Mol Cell* **32**: 150–158.

Raupach, B., Peuschel, S.-K., Monack, D.M., and Zychlinsky, A. (2006) Caspase-1-mediated activation of interleukin-1beta (IL-1beta) and IL-18 contributes to innate immune defenses against *Salmonella enterica* serovar Typhimurium infection. *Infect Immun* **74**: 4922–4926.

Richter, E., Venz, K., Harms, M., Mostertz, J., and Hochgräfe, F. (2016) Induction of macrophage function in human THP-1 cells is associated with rewiring of MAPK signaling and activation of MAP3K7 (TAK1) protein kinase. *Front Cell Dev Biol* **4**: 21.

Rivera, A., Siracusa, M.C., Yap, G.S., and Gause, W.C. (2016) Innate cell communication kick-starts pathogen-specific immunity. *Nat Immunol* **17**: 356–363.

Ruscitti, P., Cipriani, P., Carubbi, F., Liakouli, V., Zazzeroni, F., Di Benedetto, P., *et al.* (2015) The role of IL-1 β in the bone loss during rheumatic diseases. *Mediators Inflamm* **2015**: 782382.

Sanjana, N.E., Shalem, O., and Zhang, F. (2014) Improved vectors and genome-wide libraries for CRISPR screening. *Nat Methods* **11**: 783–784.

Schmid-Burgk, J.L., Gaidt, M.M., Schmidt, T., Ebert, T.S., Bartok, E., and Hornung, V. (2015) Caspase-4 mediates non-canonical activation of the NLRP3 inflammasome in human myeloid cells. *Eur J Immunol* **45**: 2911–2917.

Schroder, K., and Tschopp, J. (2010) The inflammasomes. *Cell* **140**: 821–832.

Selan, L., Papa, R., Ermocida, A., Cellini, A., Ettorre, E., Vrenna, G., *et al.* (2017) Serratiopeptidase reduces the invasion of osteoblasts by *Staphylococcus aureus*. *Int J Immunopathol Pharmacol* **30**: 423–428.

Shimada, T., Park, B.G., Wolf, A.J., Brikos, C., Goodridge, H.S., Becker, C.A., *et al.* (2010) *Staphylococcus aureus* evades lysozyme-based peptidoglycan digestion that links phagocytosis, inflammasome activation, and IL-1 β secretion. *Cell Host Microbe* **7**: 38–49.

Simanski, M., Rademacher, F., Schröder, L., Gläser, R., and Harder, J. (2016) The Inflammasome and the Epidermal Growth Factor Receptor (EGFR) Are Involved in the *Staphylococcus aureus*-Mediated Induction of IL-1 α and IL-1 β in Human Keratinocytes. *PLoS ONE* **11**: e0147118.

Sokolovska, A., Becker, C.E., Ip, W.K.E., Rathinam, V.A.K., Brudner, M., Paquette, N., *et al.* (2013) Activation of caspase-1 by the NLRP3 inflammasome regulates the NADPH oxidase NOX2 to control phagosome function. *Nat Immunol* **14**: 543–553.

Sollberger, G., Strittmatter, G.E., Garstkiewicz, M., Sand, J., and Beer, H.-D. (2014) Caspase-1: the inflammasome and beyond. *Innate Immun* **20**: 115–125.

Spano, A., Barni, S., and Sciola, L. (2013) PMA withdrawal in PMA-treated monocytic THP-1 cells and subsequent retinoic acid stimulation, modulate induction of apoptosis and appearance of dendritic cells. *Cell Prolif* **46**: 328–347.

Strowig, T., Henao-Mejia, J., Elinav, E., and Flavell, R. (2012) Inflammasomes in health and disease. *Nature* **481**: 278–286.

Syed, A.K., Reed, T.J., Clark, K.L., Boles, B.R., and Kahlenberg, J.M. (2015) *Staphylococcus aureus* phenol-soluble modulins stimulate the release of proinflammatory cytokines from keratinocytes and are required for induction of skin inflammation. *Infect Immun* **83**: 3428–3437.

Tong, S.Y.C., Davis, J.S., Eichenberger, E., Holland, T.L., and Fowler, V.G. (2015) *Staphylococcus aureus* Infections: epidemiology, pathophysiology, clinical manifestations, and management. *Clin Microbiol Rev* **28**: 603–661.

Trouillet-Assant, S., Lelièvre, L., Martins-Simões, P., Gonzaga, L., Tasse, J., Valour, F., *et al.* (2016) Adaptive processes of *Staphylococcus aureus* isolates during the progression from acute to chronic bone and joint infections in patients. *Cell Microbiol* **18**: 1405–1414.

Tuscherr, L., Medina, E., Hussain, M., Völker, W., Heitmann, V., Niemann, S., *et al.* (2011) *Staphylococcus aureus* phenotype switching: an effective bacterial strategy to escape host immune response and establish a chronic infection. *EMBO Mol Med* **3**: 129–141.

Valour, F., Trouillet-Assant, S., Riffard, N., Tasse, J., Flammier, S., Rasigade, J.-P., *et al.* (2015) Antimicrobial Activity against Intraosteoblastic *Staphylococcus aureus*. *Antimicrob Agents Chemother* **59**: 2029–2036.

Viganò, E., Diamond, C.E., Spreafico, R., Balachander, A., Sobota, R.M., and Mortellaro, A. (2015) Human caspase-4 and caspase-5 regulate the one-step non-canonical inflammasome activation in monocytes. *Nat Commun* **6** <https://www.ncbi.nlm.nih.gov/pmc/articles/PMC4640152/>. Accessed October 28, 2019.

Vladimer, G.I., Marty-Roix, R., Ghosh, S., Weng, D., and Lien, E. (2013) Inflammasomes and host defenses against bacterial infections. *Curr Opin Microbiol* **16**: 23–31.

Vuong, C., Yeh, A.J., Cheung, G.Y.C., and Otto, M. (2016) Investigational drugs to treat methicillin-resistant *Staphylococcus aureus*. *Expert Opin Investig Drugs* **25**: 73–93.

Wang, R., Braughton, K.R., Kretschmer, D., Bach, T.-H.L., Queck, S.Y., Li, M., *et al.* (2007) Identification of novel cytolytic peptides as key virulence determinants for community-associated MRSA. *Nature Medicine* **13**: 1510–1514.

Wright, K.M., and Friedland, J.S. (2004) Regulation of chemokine gene expression and secretion in *Staphylococcus aureus*-infected osteoblasts. *Microbes Infect* **6**: 844–852.

Yoshida, K., Okamura, H., Hiroshima, Y., Abe, K., Kido, J.-I., Shinohara, Y., and Ozaki, K. (2017) PKR induces the expression of NLRP3 by regulating the NF- κ B pathway in *Porphyromonas gingivalis*-infected osteoblasts. *Exp Cell Res* **354**: 57–64.

Zaki, M.H., Man, S.M., Vogel, P., Lamkanfi, M., and Kanneganti, T.-D. (2014) Salmonella exploits NLRP12-dependent innate immune signaling to suppress host defenses during infection. *Proc Natl Acad Sci USA* **111**: 385–390.

Zhu, X., Zhang, K., Lu, K., Shi, T., Shen, S., Chen, X., *et al.* (2019) Inhibition of pyroptosis attenuates *Staphylococcus aureus* -induced bone injury in traumatic osteomyelitis. *Annals of Translational Medicine* 7 <http://atm.amegroups.com/article/view/25113>. Accessed November 3, 2019.

Figure legends

Figure 1. Caspase-1 activation and IL-1 β release triggered in human osteoblasts-like MG-63 cells

A. MG-63 cells were incubated in 12-well plates. Afterwards, cells were primed for 2 h with LPS (1 μ g/mL) and stimulated with ATP (5 mM) for 15 min. Six hours after the beginning of the treatment cells together with cell-culture supernatants were diluted in RIPA lysis buffer. Protein samples were prepared in 5 x SDS-PAGE sample loading buffer. Detection of 45-kDa pro-caspase-1 in MG-63 cells by Western blot analysis was performed using anti-caspase-1 antibody (AdipoGen) as described in Experimental procedures. The protein load was verified with anti-tubulin antibody. Three independent assays were performed.

B, C. MG-63 or THP1 cells were incubated in 12-well plates. Afterwards, cells were primed for 2 h with LPS (1 μ g/mL) and stimulated with ATP (5 mM) for 15 min. THP1 were treated with PMA before LPS+ATP treatment as described above. Two or six hours after the beginning of the treatment cell supernatants were collected, centrifuged, and the level of IL-1 β was determined by a commercial sandwich-ELISA (Thermofischer Life Technologies, INVITROGEN 88-7261) as described in Experimental procedures. The sensitivity of IL-1 β detection by ELISA is 2 pg/mL.

Supernatants of THP-1+LPS+ATP were diluted 1:5. The values are presented as concentrations in pg/mL. Four independent assays were performed. The differences among the groups were assessed by analysis of variance (ANOVA). Tukey's Honestly Significant Difference test was applied for comparison of means between the groups. $P < 0.05$ (*) and $P < 0.01$ (**) were considered to be significant. The values are expressed as means \pm standard deviation (\pm SD).

Figure 2. Generation of *CASP1*^{-/-} MG-63 cells using the CRISPR-Cas9 gene editing system

A. Scheme showing the generation of *CASP1*^{-/-} MG-63 cells targeting exon 2 of the *CASP1* gene (Sequence ID NG 029124.2).

B. WT MG-63 or *CASP1*^{-/-} MG-63 cells were incubated in 12-well plates. Cells were then detached by trypsin treatment and cell pellets were obtained by centrifugation. Protein samples were prepared in 5 x SDS-PAGE sample loading buffer. Detection of 45-kDa pro-caspase-1 in WT MG-63, *CASP1*^{-/-} MG-63 G2, *CASP1*^{-/-} MG-63 B9 and *CASP1*^{-/-} MG-63 C3 cells by Western blot analysis using anti-caspase-1 antibody (AdipoGen) was performed as described in Experimental procedures. Three independent assays were performed.

Figure 3. Transmission electron microscopy analysis of MG-63 cells infected with *S. aureus* MW2

Transmission electron micrographs of MG-63 cells infected with MW2 strain at MOI 50:1 for indicated time points. MG-63 cells were fixed as described in Experimental procedures. The pellets were mixed with 3% agar in sodium cacodylate, embedded in Epon-Araldite-DMP30 resin mixture and polymerized for 48 h. Sections were cut in Leica ultra microtome, stained with uranyl acetate and were analyzed with JEOL 1400 Electron Microscope (Jeol, Tokyo, Japan). Images were digitally captured with GATAN Orius camera (Digital Micrograph Software). Magnification x12,000, scale bar: 1 μ m.

Figure 4. NLRP3 protein expression, speck-like aggregate formation and IL-1 β secretion by WT MG-63 vs *CASP1*^{-/-} MG-63 cells exposed to *S. aureus*

A. Analysis of mRNA levels of NLRP3 in WT MG-63, *CASP1*^{-/-} MG-63 G2 cells. WT MG-63 and *CASP1*^{-/-} MG-63 G2 cells were treated with 1 mg/mL ATP for 30 min, then with 5 mg/mL of nigericin for 3 h. NLRP3 mRNA level was measured by RT-qPCR. Expression of genes was normalized to the expression of housekeeping genes GAPDH and PPIA. P < 0.05 (*)

B. WT MG-63 or *CASP1*^{-/-} MG-63 G2 cells were exposed to *S. aureus* LAC (USA300) for 2 h. Following fixation and permeabilization of cells, NLRP3 expression at the protein level was determined by FACS using Rat Anti-Human NLRP3 Alexa Fluor® 488-conjugated Monoclonal Antibody or isotype control antibody (blue

colour) per 10^6 cells. NLRP3 protein expression of untreated (red colour) or infected (black colour) cells were analyzed with an Accuri C6 flow cytometer. Data were collected from 20,000 cells, and analyzed with CFlow software (Becton Dickinson). Cells are analyzed using FSC-A x SSC-A plot. The major density of events is captured by the gate.

The events that represent debris, cell fragments and pyknotic cells are eliminated. Values shown on the right side of the graph refer to the respective mean fluorescence intensities (MFIs). Double arrow shows the shift between the NLRP3 expression of non-infected control cells (red line) and cells infected with *S. aureus* at MOI 50:1 (black line). Three independent assays in triplicate were performed.

C, D WT MG-63 or *CASP1*^{-/-} MG-63 cells were exposed to 1 $\mu\text{g}/\text{mL}$ LPS for 30 min and to 5 mM ATP for 15 min (LPS+ATP) (D) or to *S. aureus* strain SA113 at MOI 50:1 for 2 h (E) followed by antibiotic treatment as described in Experimental procedures. Six hours post-infection or 6 h after the beginning of LPS+ATP treatment cell supernatants were collected, centrifuged and the level of IL-1 β was determined by a commercial sandwich-ELISA (Thermofischer Life Technologies) as described in Experimental procedures. The values are presented as concentrations in pg/mL. Three independent assays were performed. The differences among the groups were assessed by the analysis of variance (ANOVA). P-values < 0.05 were considered to be significant. Tukey's Honestly Significant Difference test was applied for comparison

of means between the groups. The values are expressed as means \pm standard deviation (\pm SD).

Figure 5. Higher number of ASC specks in *CASP1*^{-/-} MG-63 G2 cells compared to WT MG-63 cells.

A. WT MG-63 or *CASP1*^{-/-} MG-63 cells were exposed to a fluorescent derivative of *S. aureus* SA113, which carries plasmid-encoded mCherry (red fluorescence, red arrows), at MOI 50:1 for 2 h followed by antibiotic treatment as described in Experimental procedures. Six hours post-infection cells were immunostained with rabbit anti PYCARD antibody (Coger France), followed by incubation with Alexa Fluor 488 labeled goat anti-rabbit antibody (Cell Signaling Ozyme) at a dilution of 1:20 for 2 h at room temperature (green staining, green arrows). Nuclear DNA was labeled with DAPI (blue staining). Samples were viewed with a Zeiss laser-scanning microscope equipped with a 63 \times plan Apo-NA 1.4 immersion objective driven by Zen software. Scale bar: 3 μ m. Three independent assays were performed.

B. WT MG-63 or *CASP1*^{-/-} MG-63 G2 cells were exposed to *S. aureus* SA113 at MOI 50:1 for 6 h. To quantify the amount of ASC-speck forming cells the number of ASC speck out of 100 cells in the culture of WT MG-63 cells vs *CASP1*^{-/-} MG-63 G2 clone was enumerated. The results from three independent experiments in triplicate were presented. *, P < 0.05, **, P < 0.01.

C. WT MG-63 or *CASP1*^{-/-} MG-63 cells were exposed to *S. aureus* MW2 strain at MOI 50:1 for 2 h followed by antibiotic treatment as described. Six hours post-infection cells were lysed with 0.05% Triton X-100 in PBS, cell lysates were plated on BHI agar, and CFU were determined after overnight incubation. CFU values were normalized to 10⁵ host cells. Experiments were performed in triplicate. Three independent assays were performed. *, P < 0.05.

Figure 6. *S. aureus* strain-dependent release of IL-1 β by infected MG-63 cells

A. WT MG-63 or *CASP1*^{-/-} MG-63 G2 cells were grown in 6-well plates, then were exposed to *S. aureus* strain SA113 at MOI 50:1 for 2 h followed by antibiotic treatment as described in Experimental procedures. After various times post-infection (6 h, 2 days, 5 days, 7, days and 11 days) cell supernatants were collected, centrifuged and the level of IL-1 β was determined by a sandwich-ELISA (Thermofischer Life Technologies) as described in Experimental procedures. The values are presented as concentrations in pg/mL. Three independent assays were performed. The differences among the groups were assessed by the analysis of variance (ANOVA). P-values < 0.05 (*) were considered to be significant. Tukey's Honestly Significant Difference test was applied for comparison of means between the groups. The values are expressed as means \pm standard deviation (\pm SD).

B. WT MG-63 cells were exposed to *S. aureus* strains LAC (USA300, red color), MW2 (USA 400, green color), SA113 (yellow color) at MOI 50:1 or killed bacteria (violet color) for 2 h followed by antibiotic treatment as described in Experimental procedures. After various times post-infection (6 h, 2 days, 5 days, 7, days and 11 days) cell supernatants were collected, centrifuged and the level of IL-1 β was determined by a commercial sandwich-ELISA (Invitrogen, France) as described in Experimental procedures. The values are presented as concentrations in pg/mL. Three independent assays were performed. The differences among the groups were assessed by analysis of variance (ANOVA). P-values < 0.05 (*) were considered to be significant. Tukey's Honestly Significant Difference test was applied for comparison of means between the groups. The values are expressed as means \pm standard deviation (\pm SD).

Figure 7. *S. aureus* phenol-soluble modulins stimulate IL-1 β release from infected osteoblasts-like MG-63 cells

A. WT MG-63 cells were exposed to wild type LAC (USA300) and its isogenic mutant LAC Δ *psma β hld* at MOI 50:1 for 2 h followed by antibiotic treatment as described in Experimental procedures. After various time post-infection (2 days and 5 days) cell supernatants were collected, centrifuged and the level of IL-1 β was determined by a sandwich-ELISA (Thermofischer Life Technologies) as described in Experimental procedures. The IL-1 β values are presented as concentrations in pg/mL. The differences among the groups were assessed by analysis of variance (ANOVA). Tukey's Honestly Significant Difference test was applied for comparison of means

between the groups. The values are expressed as means \pm standard deviation (\pm SD). P-values < 0.05 (*) were considered to be significant. Three independent assays were performed.

B. MG-63 cells were exposed to USA300 LAC (pTX Δ 16), which carries the control plasmid, the deletion mutant LAC Δ *psma β hld* (pTX Δ 16) and the complemented strains expressing the four PSM α peptides (LAC Δ *psma β hld*-pTX Δ α 1-4), the two PSM β peptides (LAC Δ *psma β hld*-pTX Δ β 1-2), or the δ -toxin (LAC Δ *psma β hld*-pTX Δ *hld*) at MOI 50:1 for 2 h followed by antibiotic treatment as described in Experimental procedures. After various times post-infection (2 days, 5 days, 7 days and 9 days) cell supernatants were collected, centrifuged and the level of IL-1 β was determined by a sandwich-ELISA (ThermoFischer Life Technologies) as describe in Experimental procedures. The values are presented as concentrations in pg/mL. The differences among the groups were assessed by analysis of variance (ANOVA). Tukey's Honestly Significant Difference test was applied for comparison of means between the groups. The values are expressed as means \pm standard deviation (\pm SD). Three independent assays were performed. P-values < 0.05 (*) were considered to be significant.

C. WT MG-63 or *CASP1*^{-/-} MG-63 cells were exposed to USA300 LAC (pTX Δ 16), which carries the control plasmid, the deletion mutant LAC Δ *psma β hld* (pTX Δ 16) and the complemented strains expressing the four PSM α peptides (LAC Δ *psma β hld*-pTX Δ α 1-4), the two PSM β peptides (LAC Δ *psma β hld*-pTX Δ β 1-2), or the δ -toxin

(LAC Δ psma β hld-pTX Δ hld) at MOI 50:1 for 2 h followed by antibiotic treatment as described. Six hours post-infection cells were lysed with 0.05% Triton X-100 in PBS, cell lysates were plated on BHI agar, and CFU were determined after overnight incubation. CFU values were normalized to 10⁵ host cells. Experiments were performed in triplicate. Three independent assays were performed.

Figure 8. Involvement of caspase-1 in bacterial clearance

A. WT MG-63 or *CASP1*^{-/-} MG-63 G2 cells were grown in 12-well plates overnight, then were exposed to *S. aureus* SA113 strain at MOI 50:1 for 2 h followed by antibiotic treatment as described. Two hours, 6 h and 24 h post-infection cells were lysed with 0.05% Triton X-100 in PBS, cell lysates were plated on BHI agar, and CFU were determined after overnight incubation. CFU values were normalized to 10⁵ host cells. Experiments were performed in triplicate. Three independent assays were performed. The data are presented as means \pm SD. Tukey's Honestly Significant Difference test was applied for comparison of means between the groups. $P < 0.01$ (**), for the comparison of the number of internalized bacteria in *CASP1*^{-/-}MG-63 cells with those in WT MG-63 cells and P -values < 0.05 (*) for the comparison of the number of internalized bacteria in *CASP1*^{-/-}MG-63 cells 6 h and 24 h post-infection were considered to be significant.

B. WT MG-63 or *CASP1*^{-/-} MG-63 cells were grown on the slides of 12-well plates overnight, then cells were exposed to a fluorescent derivative of strain *S. aureus*

SA113 fluorescent, which carries plasmid-encoded mCherry (red fluorescence), at MOI 50:1 for 2 h followed by antibiotic treatment as described. Six hours and 24 h post-infection cells were stained with rabbit anti-PYCARD antibody (Coger France), followed by incubation with Alexa Fluor 488 labeled goat anti-rabbit antibody (Cell Signaling Ozyme) at a dilution of 1:50 for 2 h at room temperature (green staining). Nuclear DNA was labeled with DAPI (blue staining). Phase contrast and fluorescent image of host cells bearing *S. aureus* were employed to demonstrate the intracellular localization of bacteria (Inserts). We have presented inset boxes, which indicate the regions of the merged images that are shown at a higher magnification on the right of each image (Zoom). Samples were viewed with a Zeiss laser-scanning microscope equipped with a 63x plan Apo-NA 1.4 immersion objective driven by Zen software. Scale bar: 3 μ m. Three independent assays were performed.

Figure 9. Three dimensional confocal microscopy imaging of *S. aureus* internalised into WT MG-63 or *CASP1*^{-/-} MG-63 cells.

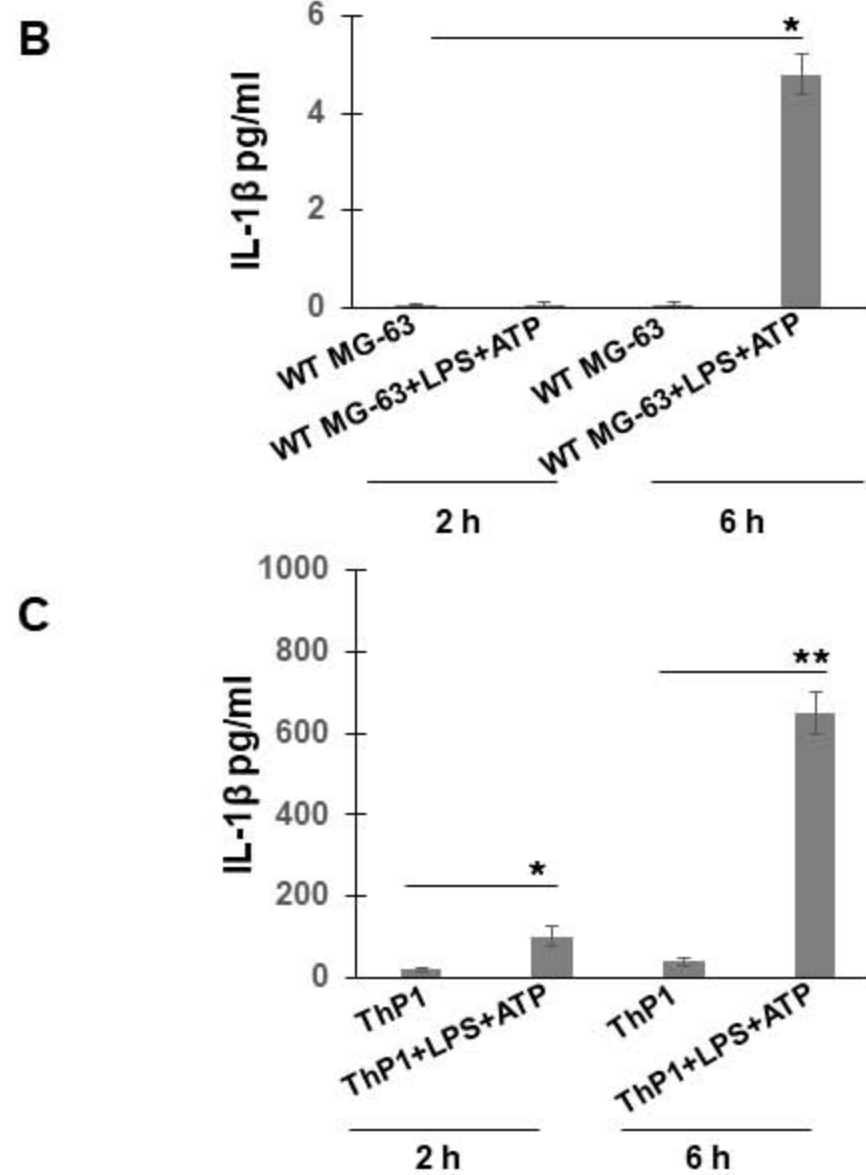
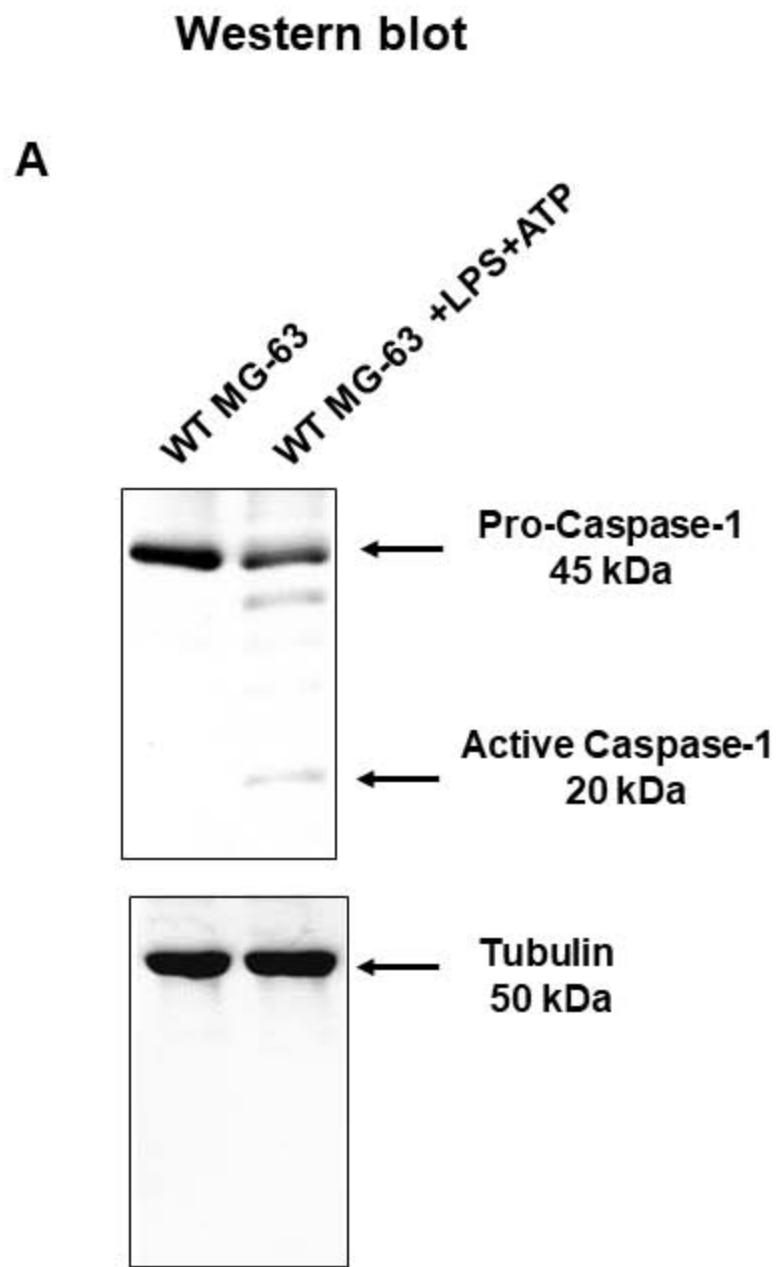
WT MG-63 or *CASP1*^{-/-} MG-63 cells were exposed to a fluorescent derivative of *S. aureus* SA113 at MOI 50:1 for 2 h followed by antibiotic treatment as described in Experimental procedures. Six hours post-infection nuclear DNA was labeled with DAPI (blue staining). Samples were viewed with a Zeiss laser-scanning microscope equipped with a 63 x plan Apo-NA 1.4 immersion objective driven by Zen software. Three independent assays were performed.

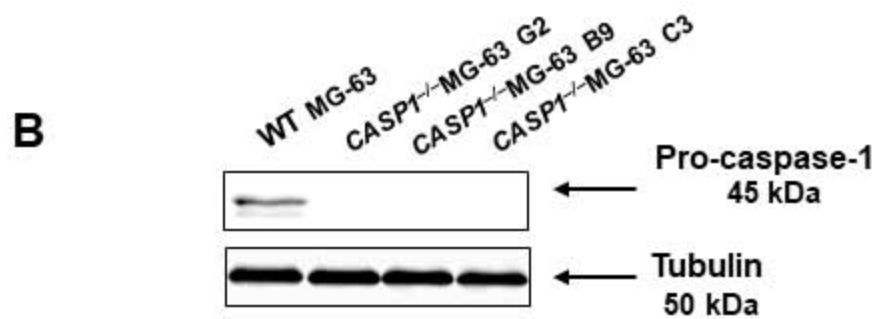
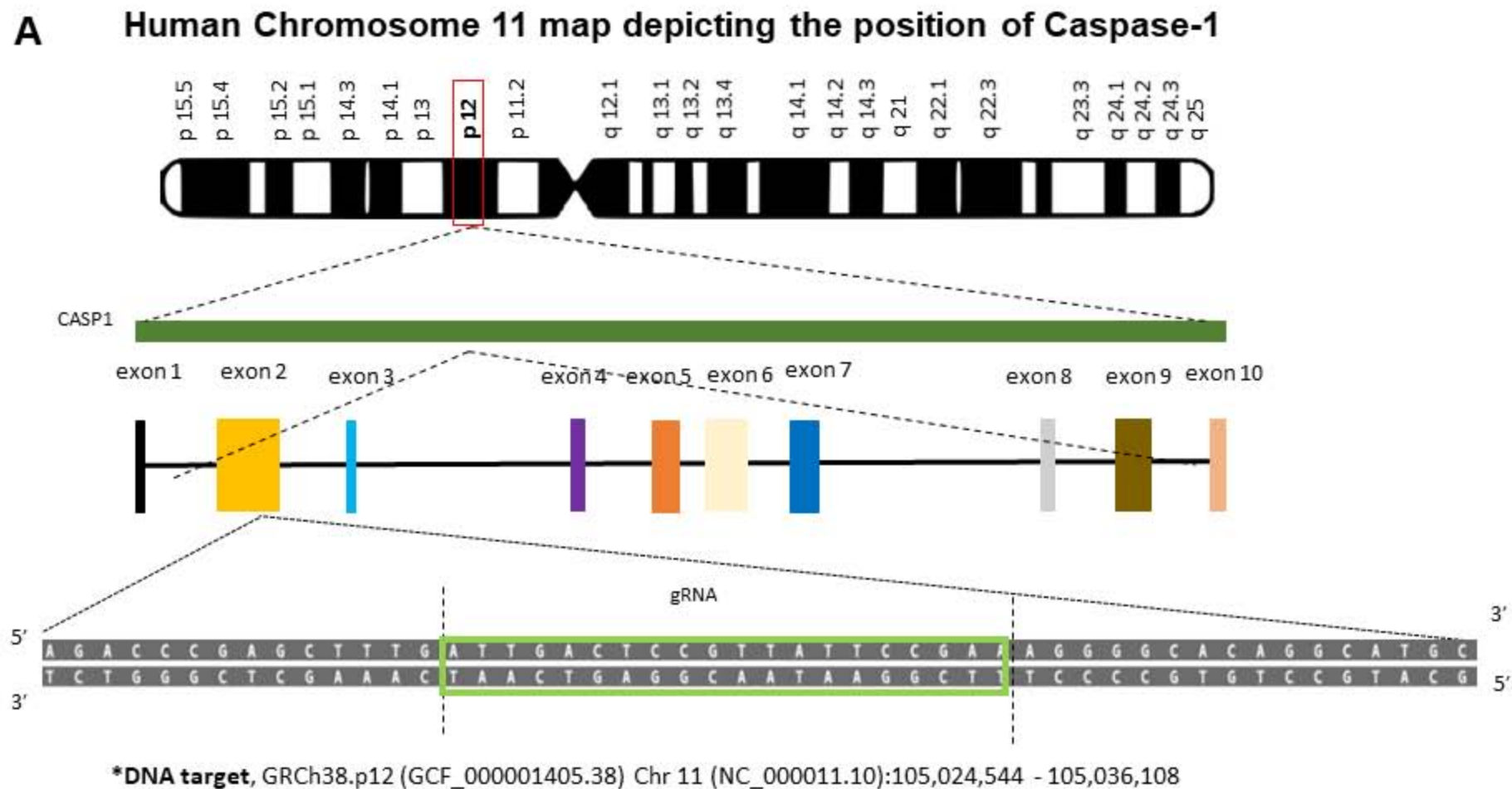
A. Multiple images were acquired in different focal planes to create a Z-stack of images (data) through the Z axis. Confocal images acquired at different “z” focal plans from the bottom to the top of the slide culture chamber in the labeled preparation. Scale bar: 3 μm .

B. Reconstituted 3D images of *S. aureus*-infected host cells were obtained by Z-stack, showing internalized *S. aureus* bacteria in the cytoplasm of infected cells.

C. Transmission electron micrographs of WT MG-63 or *CASP1*^{-/-} MG-63 G2 cells infected with SA113 strain at MOI 50:1 for 6 h. Cells were fixed as described in Experimental procedures. The pellets were mixed with 3% agar in sodium cacodylate, embedded in Epon-Araldite-DMP30 resin mixture and polymerized for 48 h. Sections were cut in Leica ultra microtome, stained with uranyl acetate and were analyzed with JEOL 1400 Electron Microscope (Jeol, Tokyo, Japan). Images were digitally captured with GATAN Orius camera (Digital Micrograph Software). Magnification x12,000, scale bar: 0,2 μm .

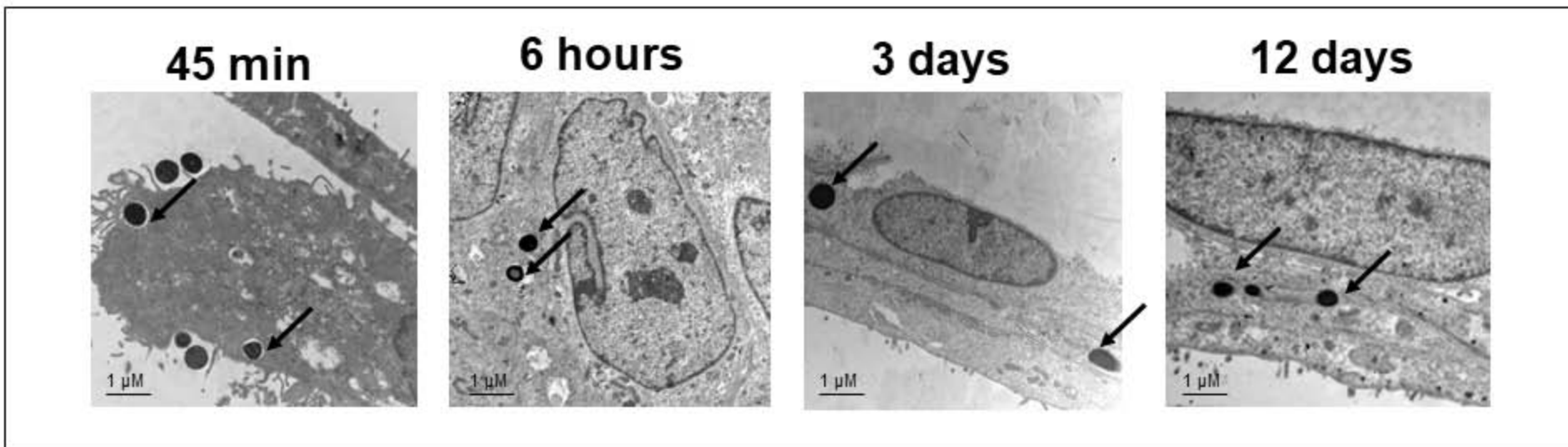
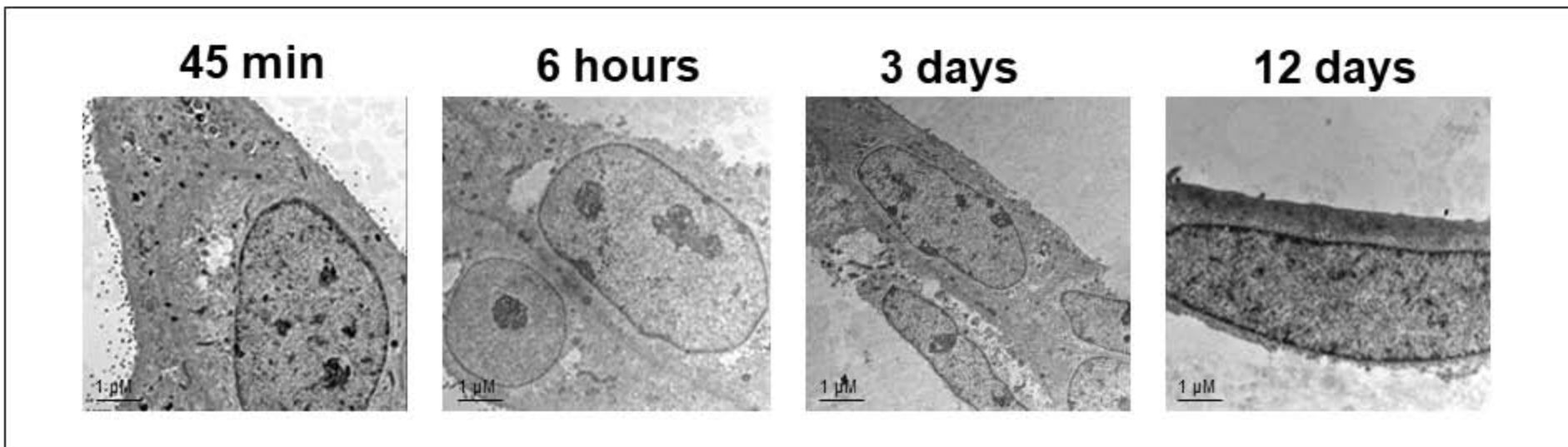
Most internalized bacteria are surrounded by phagosomal/lysosomal membranes (red arrows), some bacteria are scattered freely in the cytosol (black arrows).



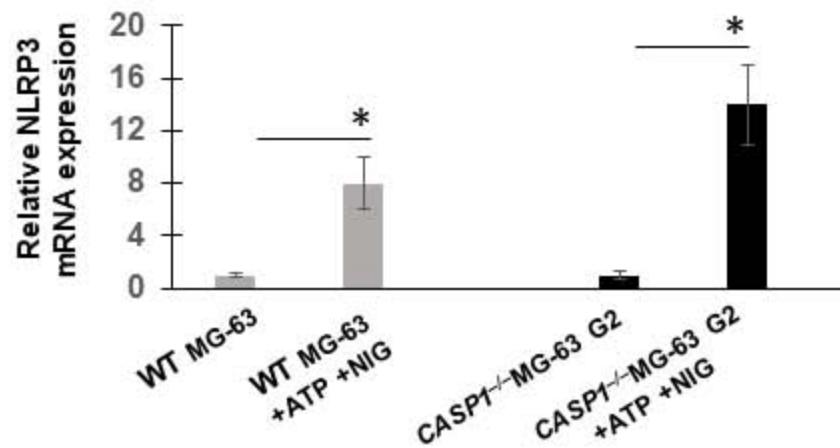


MG-63 cells +
S. aureus

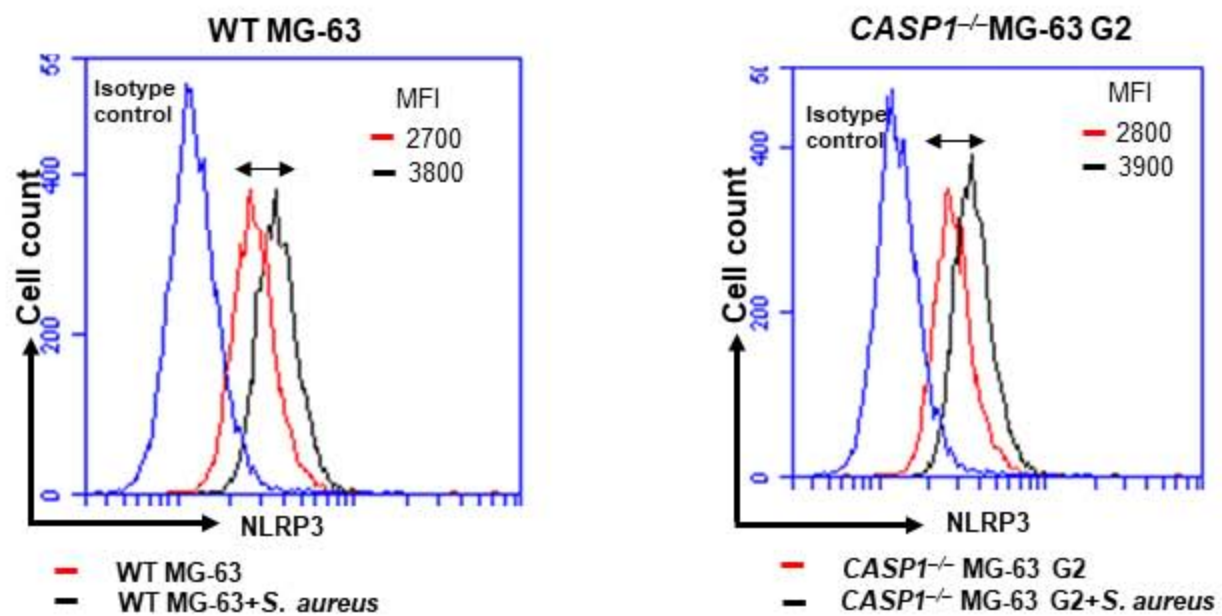
Control MG-63 cells



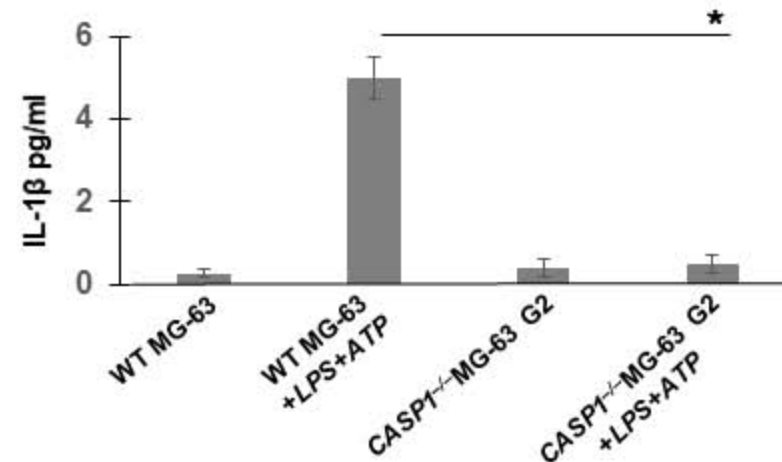
A



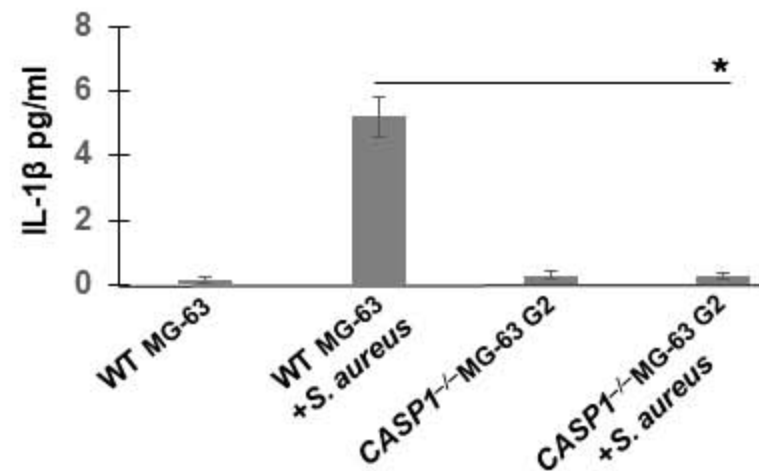
B

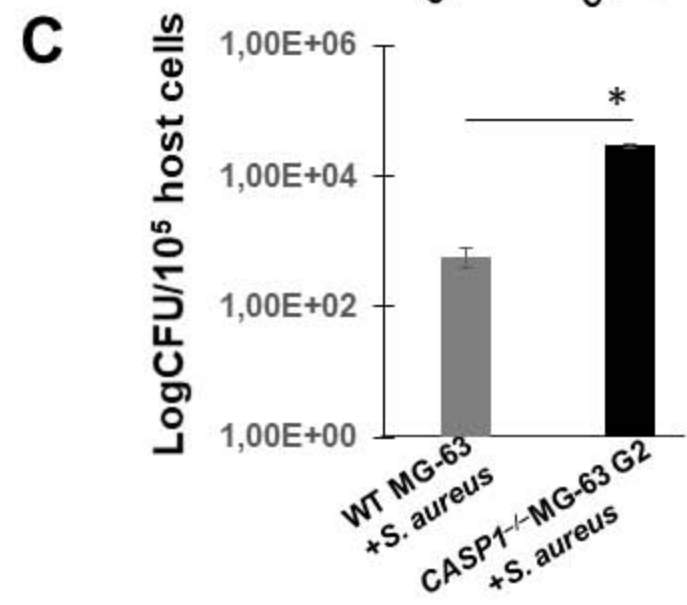
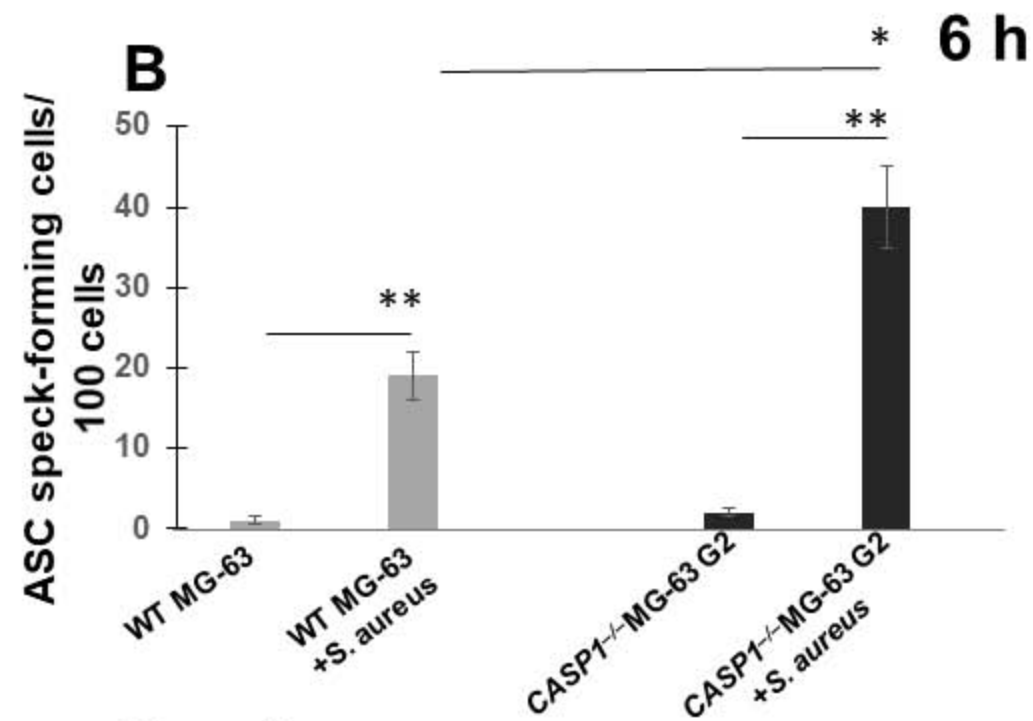
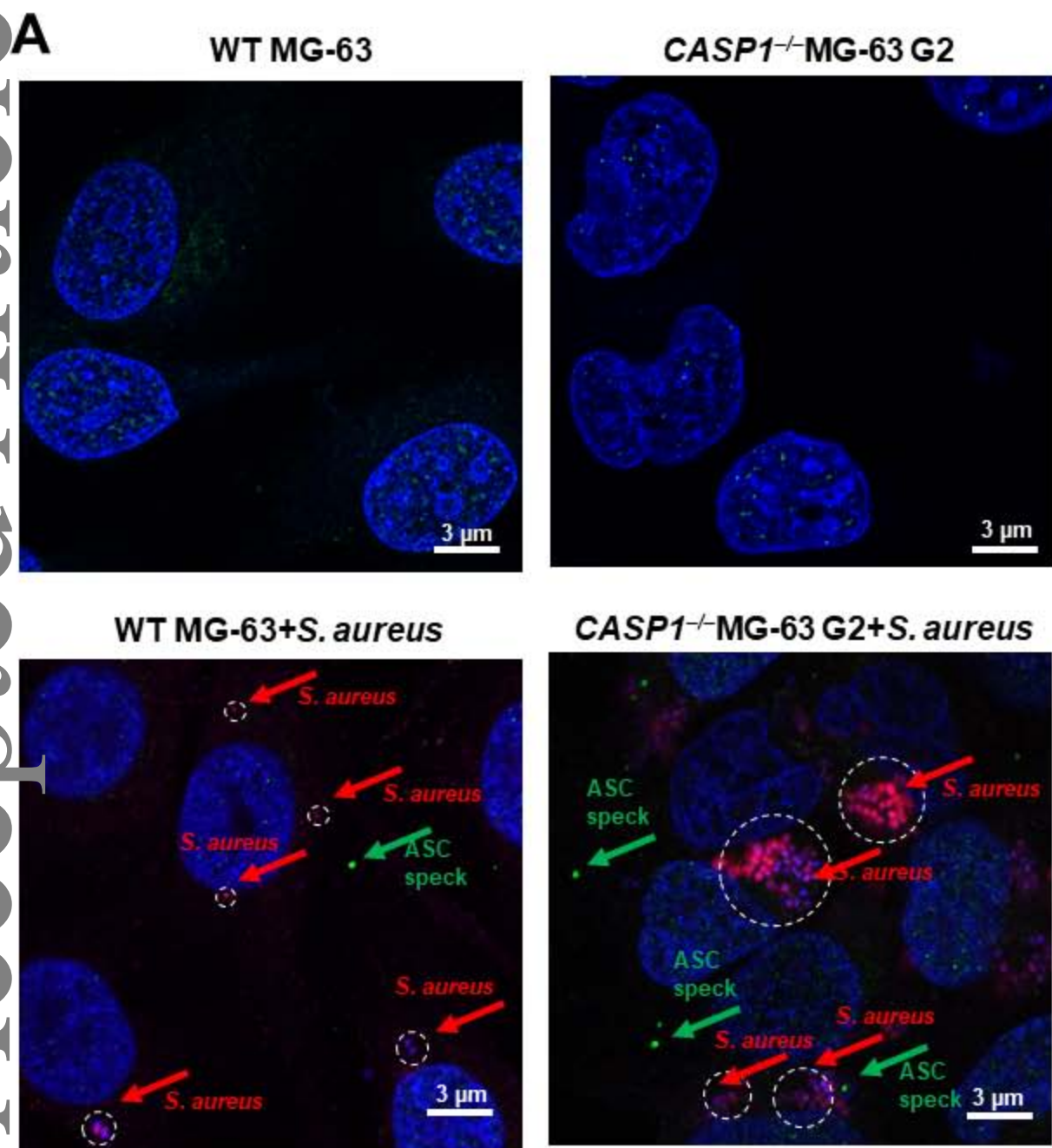


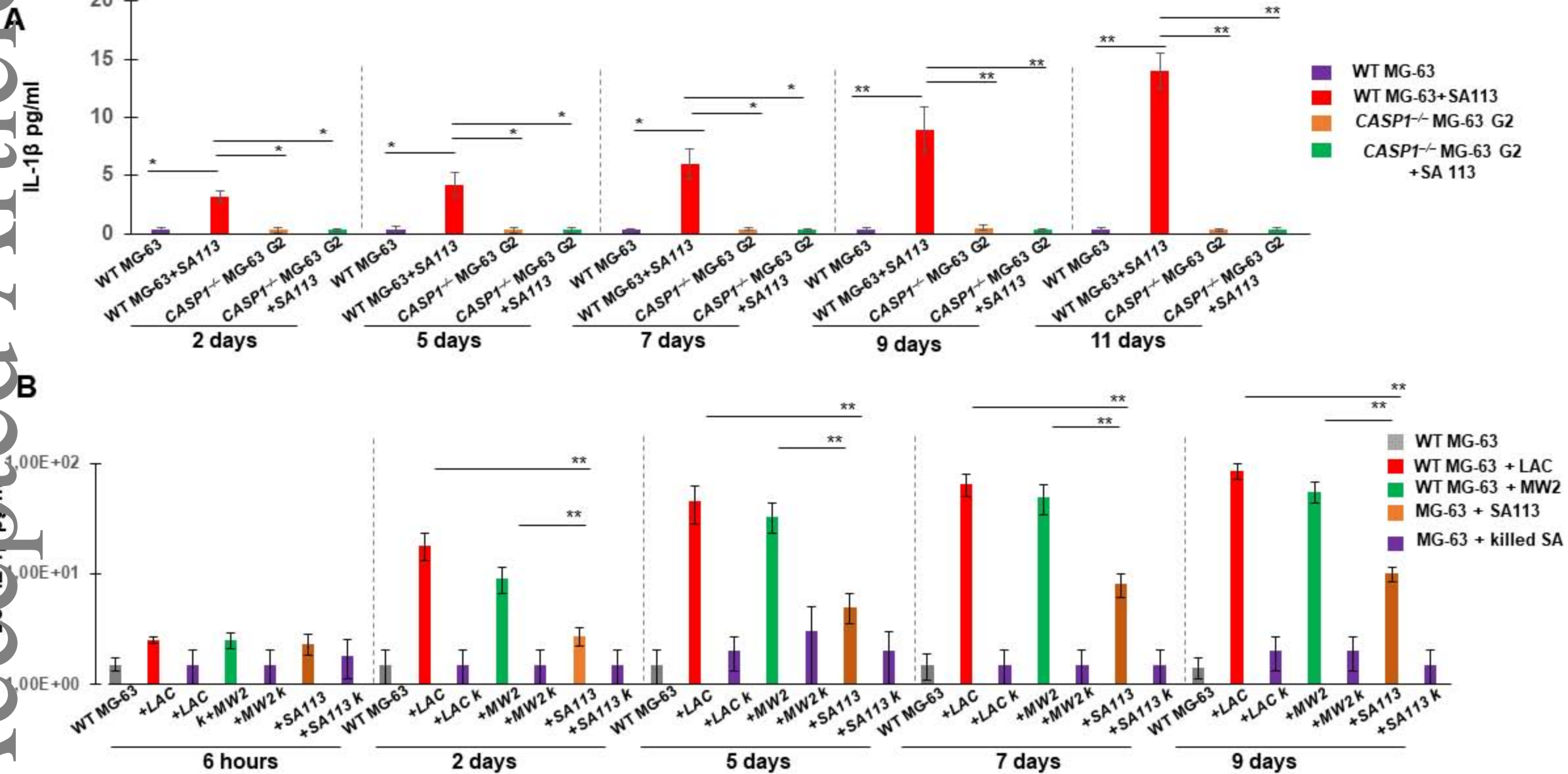
C

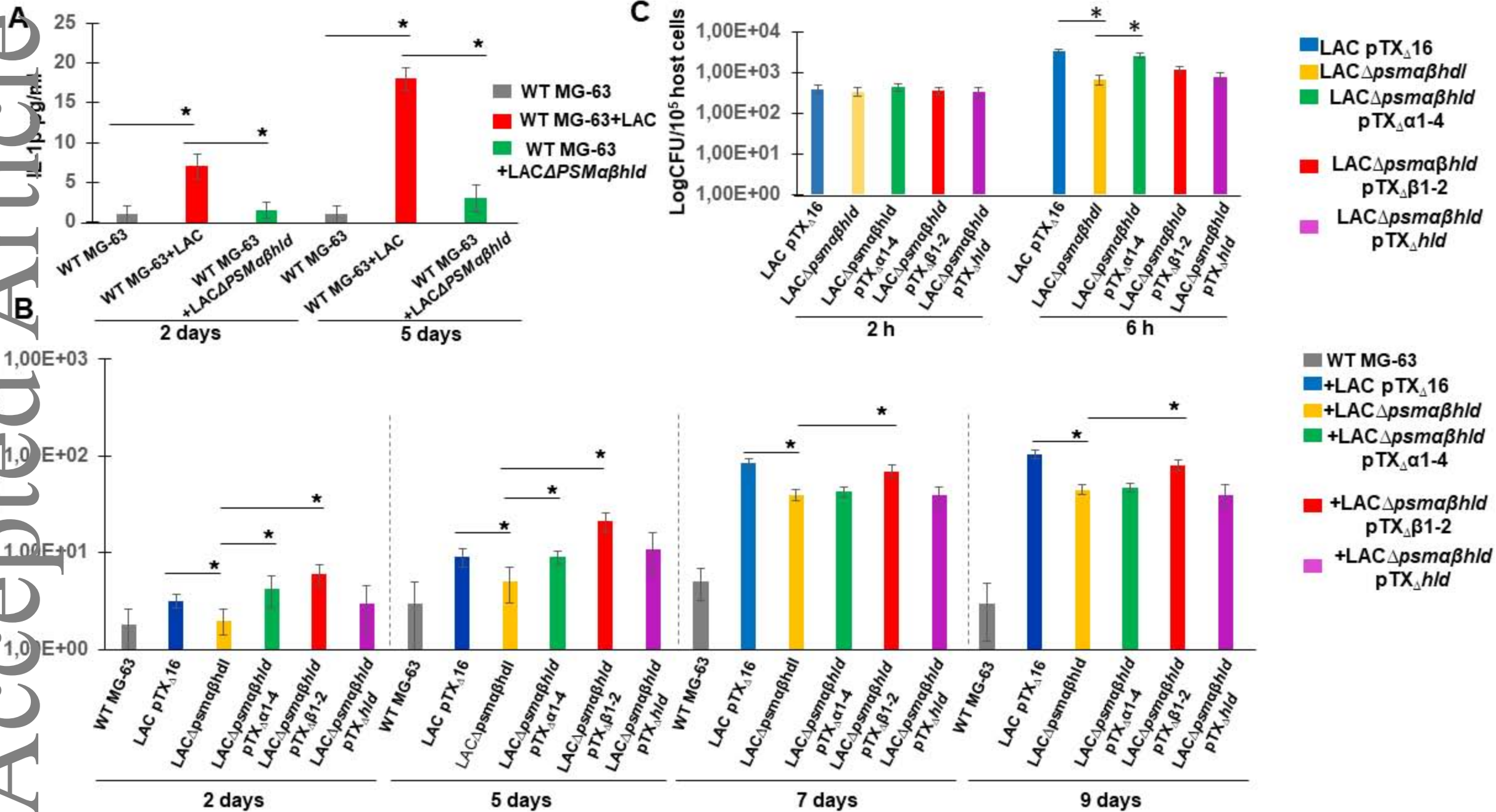


D

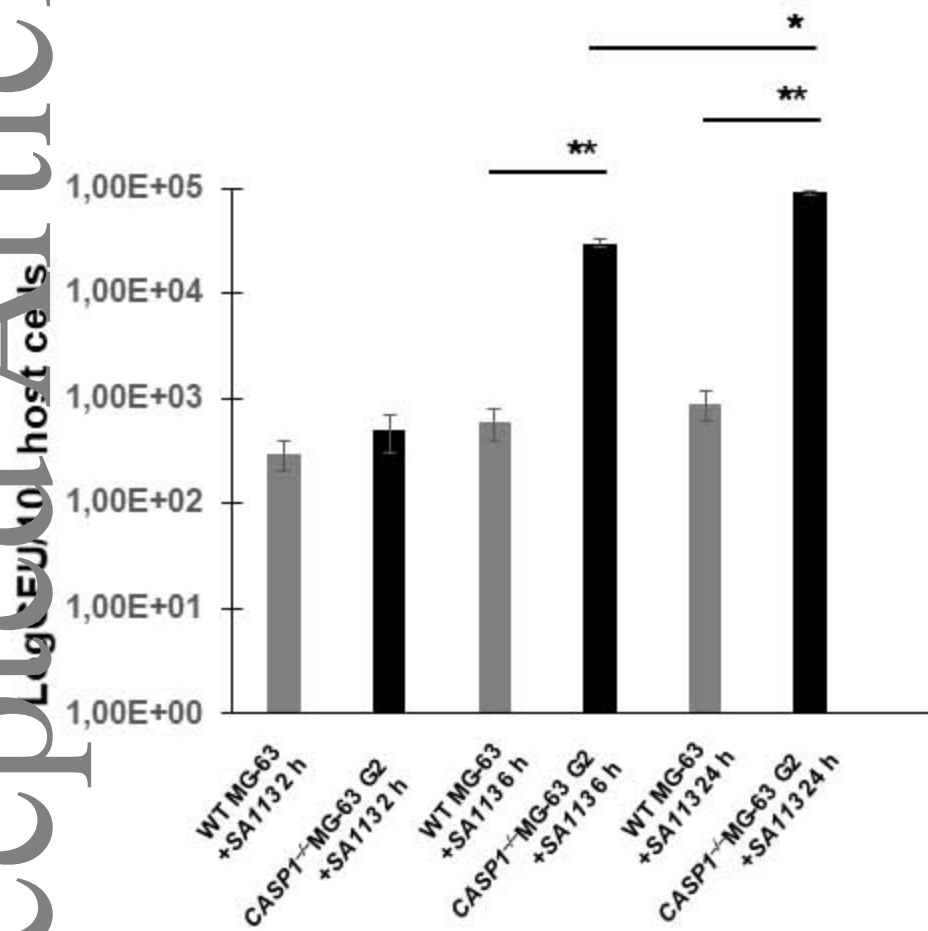








A



B

